Catalysis Today 421 (2023) 114217

Contents lists available at ScienceDirect

Catalysis Today

journal homepage: www.elsevier.com/locate/cattod

Electrode and cell design for CO_2 reduction: A viewpoint

Claudio Ampelli *, Francesco Tavella, Daniele Giusi, Angela Mercedes Ronsisvalle, Siglinda Perathoner, Gabriele Centi *

Department of Chemical, Biological, Pharmaceutical and Environmental Sciences (ChiBioFarAm) – University of Messina, ERIC aisbl and CASPE/INSTM, V.le F. Stagno d'Alcontres 31, 98166 Messina, Italy

ARTICLE INFO

Keywords:
CO_2RR
Reactor design
Electrode design
GDE
Zero-gap cell
EIS

ABSTRACT

The electrocatalytic reduction of carbon dioxide (CO_2RR) is a crucial technology to develop the decarbonisation strategy for carbon circularity and producing solar fuels substituting fossil fuels. This viewpoint discusses the role of the electrode and reactor design as the main factor in determining the performance of CO_2RR, at least under reaction conditions relevant to industrial scalability, evidencing the need to overturn the current strategic vision focused more on improving the characteristics of the electrocatalytic materials. Many parameters characterising the performances (such as Faradaic efficiency, carbon selectivity and potential onset, besides the current density) are strongly influenced and typically dominated (under relevant conditions) by the effective population of adspecies on the electrode surface, which is, in turn, related to mass control and transport resistances, local pH changes, multiphase boundaries, wettability and other aspects. Even the preliminary screening of the catalysts could be incorrect, not operating under representative conditions, and thus without properly choosing the electrode and reactor. Advanced electrode/reactor designs, e.g., based on gas-diffusion electrodes (GDEs) that avoid having a liquid electrolyte (zero-gap design), are necessary to improve CO_2RR scalability to industrial applications. Even in situ catalyst nanoparticle reconstruction may depend on these aspects. Electrochemical characterization methods like electrochemical impedance spectroscopy (EIS) are the right approach to study electrocatalytic reactions, providing crucial indications on the effective controlling elements that determine the electrocatalyst/electrode performances.

1. Introduction

The electrocatalytic reduction of carbon dioxide (CO_2) is a promising decarbonisation strategy for carbon circularity [1,2] and the development of solar fuels substituting fossil fuels [3]. The CO_2 reduction reaction (CO_2RR) gives rise to a range of products [4–10], from simple two-electron reductions (CO and HCOOH formation) to more complex electrocatalytic syntheses such as the $6e^-$ reduction to methanol or even more challenging paths involving C-C bond formation as the formation of ethanol and higher alcohols (isopropanol), light olefins, or acids such as acetic and oxalic acids. The ability to control the reaction's selectivity is thus a major issue from the application perspective. There is a debate about the preferable products of CO_2 reduction. More straightforward two-electron reduction typically allows higher current densities but, at the same time, produces chemicals not directly usable. They should be further downstream processed, making these routes (from reactants to the final product) not necessarily preferable in terms of energy efficiency and cost [11,12]. CO_2RR technologies enable carbon circularity, particularly in energy-intensive industries [13,14] and are crucial for an *e*-chemistry. The latter term indicates chemical production based on renewable energy sources and alternative C-sources to the direct use of fossil fuels [15–17].

The literature on CO_2RR principally focuses on developing selective electrocatalysts for different reactions. They are based on nano-dimensional metals/metal oxides able to activate the inert and stable molecule of CO_2 and address the selectivity towards specific compounds [18–25]. The design criteria for optimising their performances are typically focused on electrocatalyst characteristics. For example, specific active sites related to defined crystalline planes or a specific nano-morphology in the metal nanoparticles were associated with a selective path. For example, (100) facets or a nanocube morphology for copper nanoparticles enhances C2 + products by electrocatalytic reduction of CO_2 [26–31]. C2 + indicate products with two or more carbon atoms. The proposed catalyst strategies to promote selectivity in CO_2RR electrocatalysts include nanoscale and hierarchical design, exposing specific

* Corresponding authors.
E-mail addresses: ampellic@unime.it (C. Ampelli), centi@unime.it (G. Centi).

https://doi.org/10.1016/j.cattod.2023.114217
Received 13 January 2023; Received in revised form 3 April 2023; Accepted 17 May 2023
Available online 18 May 2023

Nomenclature

AEM	anion exchange membrane.
C2 +	chemicals with two or more carbon atoms.
CA	chronoamperometry.
CE	counter electrode.
CO_2RR	CO_2 reduction reaction.
CV	cyclic voltammetry.
EIS	electrochemical impedance spectroscopy.
FE	Faradaic efficiency.
GDE	gas-diffusion electrode.
GDL	gas-diffusion layer.
HER	hydrogen evolution reaction.
NP	nanoparticle.
OER	oxygen evolution reaction.
PEM	proton-exchange membrane.
PTFE	polytetrafluoroethylene.
RE	reference electrode.
SHE	standard hydrogen electrode.
WE	working electrode.

facets, quantum confinement, doping, alloying, and defect engineering. These strategies share a common characteristic: controlling the catalyst's electronic and geometric properties is decisive in determining CO_2RR paths and selectivity. Theoretical calculations typically support these indications. Fig. 1 summarises the catalyst design strategies for the heterogeneous CO_2RR process [32]. The electronic structure of a catalyst surface determines the overpotential and selectivity of the CO_2RR by influencing the binding energies of reaction intermediates. The geometric structure is typically related to the catalytic site density and arrangement, controlling product selectivity and current density. Several factors, such as grain boundary defects or doping, may influence electronic and geometric structures.

Although Fig. 1 simplifies the many literature studies on CO_2RR, it shows that the research is focused mainly on the electrocatalyst characteristics to control conversion paths and performances. The electrocatalytic reactor design and engineering and the choice of operative conditions are scarcely considered in the literature. However, common experimental practice remarks how they are crucial in determining electrocatalytic performance and behaviour.

On the other hand, it has been reported that the electrocatalytic behaviour is determined by surface structure (at nano- and mesoscale) and factors such as electrolyte effects (pH, buffer strength, ion effects), mass transport conditions and three-phase boundaries, e.g. the region at the interface between solid, liquid, and gas [33–42]. The design and engineering of the reactor determine such aspects. However, the connection between reactor configuration and three-phase boundaries or electrocatalyst-electrolyte interface is typically not considered, and the role of the reactor configuration in determining the performances is analysed in a few studies, particularly concerning the industrialisation of the processes [43–48].

The underlying assumption is that the reactor design only concerns process engineering. It follows the development of the "optimal" electrocatalysts, assumed as the main factor determining the behaviour and selective conversion paths. It is often assumed that the electrocatalytic reactor design is essential to minimise the process resistances and, thus, to enhance the current density mainly. We showed that the electrocatalytic reactor configuration influences the surface population of CO_2, intermediates and hydrogen species which can induce the selective formation of C2 + products (with Faradaic selectivities up to over 60%) even on electrocatalysts such as Pt which typically does not form C2 + products [49]. Thus, transformation paths depend on the reactor design and related elements rather than the electrocatalyst itself.

In addition, the cathode where CO_2RR occurs is typically considered an independent element from the anode and reactor. The nature of the anodic reaction is often not considered, and even sacrificial reactions are sometimes used. On the contrary, the anodic and cathodic processes are strongly coupled, being in series in a closed circuit that involves ionic and electronic transport through the membrane, electrolyte, connecting wires, and other aspects. The potential and current distribution at the cathode are determined by both the anode and reactor design. Furthermore, the potential and current distributions are far from homogeneous over all the electrode surface. These effects are probably minimal when small-size (lab-scale) electrodes are used, as used mainly in the literature. They are also neglected as attention is only focused on the cathode behaviour. However, they become crucial for the overall behaviour in larger-size electrodes/reactors. They are considered in the scale-up and industrialisation of the electrocatalytic processes.

The formation of gas bubbles can strongly influence the interface at the electrocatalyst-electrolyte boundary. Besides to hydrophobic character of the electrode, the adherence, size, etc. of these gas bubbles depend on the micro-fluidodynamic aspects of the electrolyte in contact with the electrode, in turn depending on the reactor design. Some of the changes in performances observed between different electrocatalysts are possibly related to these aspects rather than other intrinsic characteristics of the electrocatalysts.

Therefore, optimising the catalyst is not the only aspect to consider, but a proper electrode and cell design is the key to raising the performance of this challenging process. From a literature survey, studies

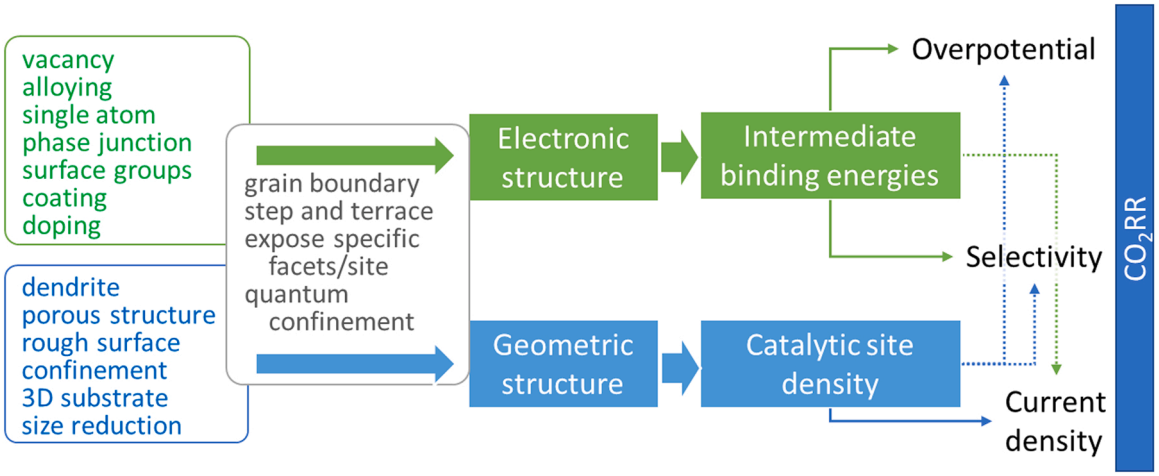

Fig. 1. Overview of catalyst design strategies for the CO_2RR. Original Figure, based on indications given in ref. [32].

focused on these aspects are somewhat limited, and the trend of interest has only recently started to increase (see Fig. 2).

The CO_2 reduction usually occurs at the electrode/electrolyte interface. It involves the adsorption/activation of CO_2 on the catalyst's surface, followed by protons and electrons multiple transfers to break the oxygen-carbon bonds and form adsorbed products. Usually, the catalyst is deposited on a conductive substrate (e.g. carbon paper or glassy carbon) to form an electrode immersed in a liquid electrolyte solution. Typically, the electrocatalytic tests are performed in an H-type cell, so called for its H-like form with two liquid compartments separated by an ion-exchange membrane, where the catalyst acts as the working electrode in the cathodic chamber for CO_2 reduction. However, these (semi-) batch systems suffer from mass transfer limitations due to the low solubility of CO_2 in aqueous media and the high availability of protons that compete to react with electrons to form hydrogen. The competition with the hydrogen evolution reaction (HER) is critical in water-based electrolytes due to both thermodynamic and kinetic reasons.

Different reactor configurations have been explored to solve the above limitations. Continuous flow-cell electrolysers should be used, especially from an industrial-scale perspective [50]. Their use is expanding, but batch-type operations are often used, such as with the H-type cell mentioned above. These batch-type operations often do not provide reliable indications [50]. However, these continuous-flow devices should be adequately designed to minimise energy losses and operate at high current densities. It is often assumed that this is not a relevant aspect to consider. Excellent Faradaic efficiencies (FEs) are reported for negligible current densities but drastically decrease at more realistic current density conditions. This aspect indicates the importance of giving attention to electrocatalytic reactor design and operating in the right conditions to provide reliable results.

Recently, we pointed out the importance of a correct electrode and cell design in CO_2 electrocatalytic reduction not only to improve mass transfer but also to address the process selectivity to the formation of more valuable compounds, such as hydrocarbons, alcohols, and other oxygenates with two or more carbon atoms (C2 +) [51]. The electrode design and adopting a proper reactor configuration can make the difference in producing selectively one product instead of others beyond the properties of the electrocatalytic material itself. Specifically, we observed that gas-phase operations, in combination with the use of gas-diffusion electrodes (GDEs), can induce a higher surface coverage of the electrode by CO_2 (or by other ad-species formed by its reduction), thus shifting the reaction pathways towards the formation of more interesting C2 + products.

In this approach, also called the electrolyte-less or zero-gap approach, the membrane is used as a solid electrolyte to close the electrical circuit between the two electrodes. Since no liquid electrolyte is employed in the cathode part, the membrane is in strict contact with the catalyst in the form of a GDE crossed through by CO_2, separating the cathodic reaction zone from the anodic part. We also reported that a Pt-based catalyst (known to be non-selective for C2 + formation) could modify its electrocatalytic behaviour if CO_2-adsorbing elements are added to the GDE [49], confirming that engineering of the electrode structure plays a fundamental role in the CO_2 reduction process.

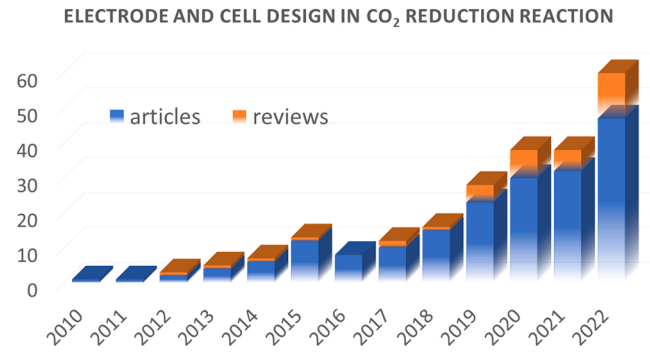

Fig. 2. Number of scientific papers published in 2010–2022 about "electrode and cell design in CO_2 reduction reaction". Data reviewed by Scopus Database (Keywords: "CO_2 reduction" AND "electrode and cell design") updated as of December 31st, 2022.

Designing the reaction zones in GDEs is also important in determining the selectivity of CO_2 reduction. Möller et al. [52] recently reported that selectivity is influenced by adjusting the structure of the electrode, suggesting a correlation between mass transport and local pH. The overall mass transport within a porous catalyst can also be modulated by regulating the wettability of the material at the microscale, influencing the transfer of protons and reducing their availability for H_2 production [53]. The type and concentration of alkali cations in the electrical double layer can primarily affect CO_2RR [54]. Large-size cations (e.g., Cs^+) enhance the activity and FE nearly independently of the catalysts.

Thus, the catalyst development should be integrated by a proper electrode and reactor design to exploit the potential viability of the electrochemical CO_2RR.

This concise viewpoint addresses the design and engineering of electrodes and reactors beyond the properties of the electrocatalyst. It will mainly focus on the role of the different reactor approaches for the electrocatalytic CO_2 reduction, ranging from the standard H-type devices to the recently more used flow cells, especially evidencing the advantages of using gas-phase systems (with no bulk electrolytes, thus also called electrolyte-less reactors [55,56]) in the place of liquid-based electrolysers. The gas-phase approach is advantageous because it provides: i) a more compact configuration, easier to scaled-up and to develop stacked electrocatalytic reactors, (ii) avoids gas diffusion problems in the liquid electrolyte, (iii) no limitations due to CO_2 solubility in the electrolyte and mass transfer, and (iv) easier recovery of liquid products. Furthermore, this contribution aims to highlight from a personal perspective the most promising solutions to move from the lab-scale to industrial implementation through pilot experimentation.

2. Electrode design

This section will not discuss the characteristics of the electrocatalysts to their performances in CO_2RR and the design criteria for their optimisation and control of the selectivity, for example, defect nature, presence of specific nanomorphologies, or type of active metal or metal-oxide. These aspects are discussed in a different contribution to this issue. Discussion is limited here to the analysis of the characteristics of the electrodes determining the mass transfer, three-phase boundary, wettability and other aspects.

2.1. *Electrode nanoengineering*

The electrode structure and characteristics, often underestimated, is crucial to guarantee the optimal contact between CO_2, protons and electrons. The electrocatalyst is typically deposited over a conductive substrate that should provide a homogeneous distribution of electrode (CO_2RR occurs over a cathodic electrode) over the entire substrate, thus avoiding, in principle, differences in the potential from different zones. The resistance in electron transport between the electrocatalyst nanoparticles (NPs) and the substrate should also be minimal and similar over the entire electrode area. Otherwise, the effective local potential at the electrocatalyst NPs could differ from particle to particle. These aspects are often assumed not relevant, particularly in lab-scale testing units. However, experience teaches that significant differences are often observed by changing the substrate characteristics. If the electrode is directly immersed in the electrolyte, CO_2 contact with the electrocatalyst is mediated by CO_2 adsorption in the electrolyte and its transport to the reactive sites. The issue of CO_2 solubility in the electrolyte is often accounted for, but less the issue of CO_2 diffusion.

In a porous electrode, which results polarised by applying the

potential, the transport of solubilised CO_2 may be limited, especially when low turbulence (Reynolds number) is present, as the typical case of most of the lab-scale electrocatalytic reactors. The concentration of CO_2 at the interface with the electrocatalyst NPs may thus not be uniform, affecting the catalytic performances.

Similar phenomena are present in the diffusion of protons at the surface of the electrocatalyst NPs. None of the above limitations should influence the performances when different electrocatalysts are compared. In heterogeneous catalysis, the verification of measuring an effective kinetic rate not limited by mass transfer is a common practice. However, as mentioned above, this is much less used in electrocatalytic tests, where additional physical transport limitations may also exist. Protocols for testing electrocatalysts and verification that none of the above limitations are present are essentially missing in the literature and discussion or benchmarking of the results [57]. Some techniques are available to have insights into these aspects as acoustic streaming [58], elaboration of linear sweep voltammetry curves to obtain intrinsic kinetic parameters [59], accurate measurements of the electrochemical effectiveness factor and the Thiele modulus [60]. However, these experiments are usually not practised in CO_2RR tests. Thus, it may not be unusual that what is attributed to intrinsic differences in the electrocatalysts is related instead to differences in the physical transport effects, resistance and non-homogeneity in electron transport, effective accessibility to electrocatalysts NPs, and related aspects.

In fuel cells, a common practice is determining the effective electroactive area of the catalyst NPs, measured by cyclic voltammetry tests [61]. The comparison of electrodes for fuel cells is incorrect without normalisation to the same electroactive area [62]. The nature of the substrate strongly affects this aspect [62]. A similar type of experiment and procedure is essentially absent in CO_2RR experiments.

Due to the dependence of the selectivity from the effective surface concentration at the electrocatalyst of CO_2 and protons [52], as well as from the local potential (depending on the nanostructure and electron flow), we may expect that not only the activity (current density) but also the FE results are influenced. The overpotential in the reaction also depends on the resistance to the flow of electrons from the substrate to the electrocatalyst NP. Then, the overpotential onset, which is often considered only an intrinsic property of the electrocatalyst nature, may also be influenced by these transport resistance aspects.

The electrode structure and its optimisation/engineering may thus be critical in determining the overall performances, even if not enough attention is given to these aspects beyond the electrocatalyst itself [45, 63].

Three general types of cathode architectures for CO_2RR have been reported (Fig. 3): (a) planar electrodes (e.g. a metal foil or glassy carbon plate), (b) porous electrodes (e.g. carbon paper or mesh), and (c) gas-diffusion electrodes (GDEs) in the two configurations, conventional and electrolyte-less (no bulk electrolyte, also called a gas-phase reactor).

Most CO_2RR studies use planar or porous electrodes [63] (Fig. 3a) because they are relatively simple to construct and change. They are immersed in a CO_2-saturated electrolyte. A reference electrode can be easily introduced to measure overpotentials. The principal limit is the dependence of the performances on the CO_2 diffusion and ionic diffusion, which inhibits measurements at high current density. 3D-type structured electrodes (Fig. 3b) increase the active electrode area, reducing overall cell voltage because lower overpotentials are necessary to obtain a suitable current density. Tests at higher current densities can provide conditions that avoid CO_2 and proton transport limitations. However, intra-electrode mass transport can become limiting at high current densities, and inhomogeneities in electron distribution are amplified. These issues are related to the complexity of the 3D-structured electrodes. They involve multiphase flow in the pores, interface interactions, and multiscale kinetics at the catalysts. It is a largely unexplored area in CO_2RR [64–66], different from PEM fuel cells and redox flow batteries [67,68]. The 3D skeleton and the interfacial conductivity determine the ohmic resistance of the 3D-structured electrode. Foams are of increasing interest as the conductive substrate. The wettability of the substrate is a crucial aspect, as commented later. Wettability and pore size dominate the intrinsic saturation/capillary-pressure relationship determining the optimal multiphase performance [69].

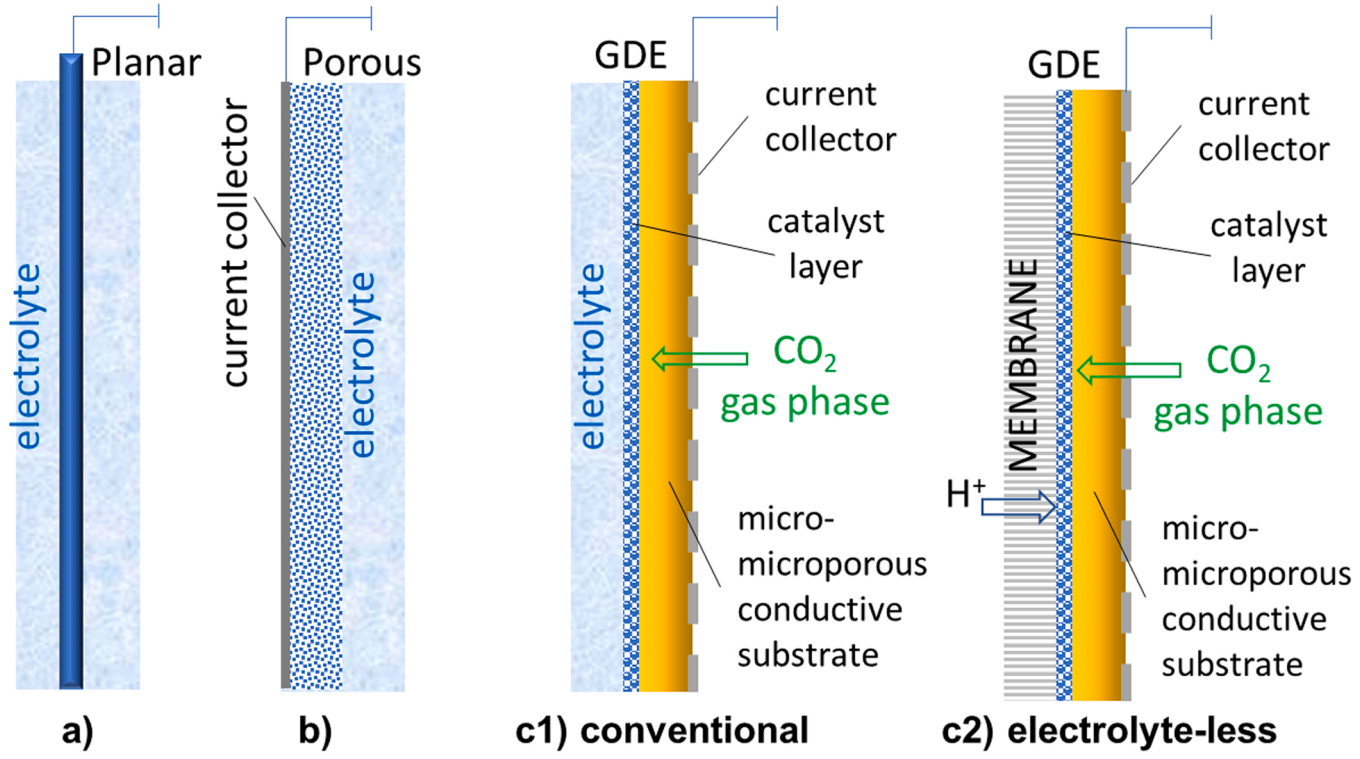

Fig. 3. Simplified schemes of (a) planar electrode, (b) porous electrode, (c) gas-diffusion electrode (GDE) in the two options for conventional electrocatalytic reactors in the presence of a bulk electrolyte and electrolyte-less configuration (gas phase).

The resistance in an electrochemical reaction depends on the electrode kinetics. The latter, in turn, depends on electrocatalyst properties but also on the conductive substrate and interface with the electrocatalyst, the type of multiphase flows within the electrode and local environments. All these aspects determine CO_2RR surface reaction rate and selectivity, rather than only the electrocatalyst [70]. Still, gaps remain in understanding aspects such as the interfacial structure of the catalysts and nanoarchitecture and impact on the electrode kinetics, particularly in CO_2RR. For example, metal-oxides or hydroxide structures formed in situ during electrocatalysis are active in CO_2RR [71,72]. However, in principle, they are poorly conductive and lead to an increase of ohmic resistance in electron transfer.

GDEs are those on which attention especially focuses recently. They generally have superior CO_2RR performance compared to planar and porous electrodes, with higher rates up to an order of magnitude due to the increased transfer rate of CO_2 to the electrode [63,73]. In GDEs, the CO_2 gas diffuses through a gas-diffusion layer (GDL) to the electrocatalyst layer, which may be or not in contact with a bulk liquid electrolyte (Fig. 3c). In the electrolyte-less configuration, the transport of the protons occurs through a membrane which separates this cathodic zone from the anodic one on the other side of the membrane. Thus, the membrane acts as both the membrane separating cathodic and anodic compartments and as a solid electrolyte to close the ionic circuit.

GDE improves CO_2RR performance by allowing a higher active surface area and lower mass-transfer resistances. However, many electrode properties are critical in determining performance, such as wettability, catalyst loading, and porosity [73]. These factors are sensitive to operating conditions and depend on the current density. The GDL must have optimal wettability, e.g. the GDL should prevent the liquid electrolyte from flooding the gas flow channel. GDL is typically a metal mesh (or foam) or a conductive porous carbon substrate (carbon cloth or felt) hydrophobically treated by chemicals such as polytetrafluoroethylene (PTFE). A dual-layer GDL formed by a macroporous and a microporous layer is also used. The catalyst layer is usually deposited by spray drying or similar methods, preparing an ink composed of the electrocatalyst, eventually deposited on conductive support such as carbon nanotubes to minimise resistances in electron transfer with the GDL and favour dispersion/stability, and an ionic binder.

Optimisation of the porosity and electrolyte fluid dynamics is important. GDE optimisation is crucial to allow high performances, even more than improving the electrocatalyst, but the engineering of the GDE should parallel that of the reactor itself. Still, few studies investigated the optimisation of GDEs for CO_2RR and their nanoengineering parallel to electrocatalytic reactor engineering [63].

An aspect still few investigated is the possibility of adding to GDL components that enhance the CO_2 adsorption and create a virtual higher partial pressure of CO_2 at the electrocatalyst, particularly in the electrolyte-less GDE configurations (Fig. 3c.2). We showed that by introducing imidazolate-based metal-organic framework (SIM-1) on GDL, it is possible to increase the performance significantly and control the selectivity in CO_2RR, enhancing the formation of C2 + products [49]. This concept could be used to develop improved GDE, which allows operating directly with diluted CO_2 concentrations. This concept could revolutionise the industrial application of direct CO_2RR electrocatalytic routes to recycle CO_2 in industrial emissions because often, the stage of carbon capture accounts for up to half of the total cost of reuse CO_2.

A critical issue is that in parallel to realising the local capture of CO_2 from the diluted stream, it is also necessary to avoid negative effects by other components present in the feed (e.g., O_2 and other molecules) eventually poisoning or reducing the efficiency of the electrocatalyst. This possibility is highly challenging but not impossible. It is necessary to design the GDE with likely additional permeoselective membranes to only CO_2 [74–76]. Fig. 4 illustrates the concept of such technology through the schematic description of an advanced photoelectrocatalytic device able to convert CO_2 from industrial emissions directly. CO_2 is transported to the catalytic layer through a GDL containing functionalities that capture and concentrate CO_2 (from diluted streams) at the catalyst surface. The cell design includes a CO_2 permeoselective membrane that prevents diffusion of other gaseous components in the industrial emission, such as O_2 and thus their contact with the electrocatalyst.

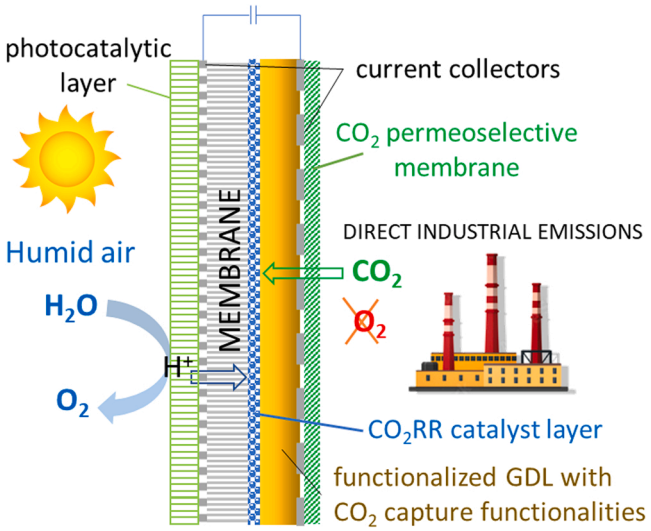

Fig. 4. The concept of an advanced photoelectrocatalytic device able to directly convert CO_2 from industrial emissions (see text). It is composed of a photocatalytic layer, which should be porous to transport photogenerated protons to a proton-conductive membrane and then to the CO_2 electrocatalyst layer. CO_2 is transported to this catalytic layer through a GDL, which contains functionalities that capture CO_2 from diluted streams and concentrate at the catalyst surface. A CO_2 permeoselective membrane prevents other components in the industrial emission, such as O_2, from arriving in contact with the electrocatalyst.

On the other side of the membrane (see Fig. 4), a porous photocatalytic layer with multiple functionalities is used to i) allow efficiently solar energy exploitation and generate charge separation (semiconductor), ii) catalytically produce O_2 and protons for water oxidation, and iii) allow the efficient transport of the photogenerated protons to the membrane in contact with the photocatalytic layer, while the electrons are transported through a collector to the cathodic part of the cell. An example is a layer of ordered TiO_2 arrays of vertically aligned nanotubes grown by anodic oxidation on perforated Ti foil (acting as electron collector) and modified by copper nanoparticles and other semiconductors (such as $BiVO_4$ or g-C_3N_4) to increase the activity with visible light components [77–79].

Given the high industrial relevance of this possibility to develop a CO_2RR technology (based on the use of a permeoselective membrane in combination with the use of photocatalytic electrodes or with PV modules to use solar energy) which directly converts the CO_2 present in industrial emissions, it surprises the minimal scientific attention given to this crucial topic of CO_2RR technology design. There are studies which combined CO_2 capture and electrochemical conversion [80]. However, the concept is different. CO_2 is captured in an amine-scrubbing step, and then the CO_2-rich amine solution is used as the electrolyte in the CO_2RR unit. However, it is not an optimal electrolyte. The concept presented in Fig. 4 instead avoids the step of CO_2 capture with the related use of an amine or similar absorption medium. Instead, it uses a functionalized membrane (part of GDE) to interface directly with the gas-phase emission. This solution has evident energy and cost advantages, although highly challenging.

2.2. The role of local concentration gradients in the electrode

CO_2RR operations at high current densities, as required from an industrial perspective, often induce critical issues of local concentration gradients [52]. For industrial applications of CO_2RR technology, long-term operation (>10.000 h, e.g. at least one year) at substantial current densities (>200 mA•cm^{-2}) should be proven to minimise the capital expenditure [81–83].

Various CO_2RR studies work at high current densities, even if sometimes too strong basic electrolytes, which may be unfeasible from an industrial perspective, were used to achieve these performances [84–86]. These electrolytes are necessary to realise the electrolyte's strong ionic conductivity and limit the electrode's gradients. Both aspects can be improved by working on the engineering of the cell and electrodes, thus allowing the achievement of high-current densities without using such critical electrolytes that ideally should have a pH close to neutrality.

The cathodic and anodic reactions in CO_2RR induce a change in the pH. In aqueous electrolytes, CO_2 adsorption equilibria are present and the concentrations of carbonate and bicarbonate ions depend on the pH. The transport properties also affect the availability of protons for CO_2 reduction. In buffered electrolytes, the local alkalisation due to insufficient HCO_3^- transport influences the selectivity for C2 + products [73, 87,88]. The active surface area and thickness of the catalytic layer were found to influence the onset potential, selectivity, stability, and activity due to mass transfer inside and outside of the electrode [87]. The catalyst selectivity and activity are highly sensitive to the local reaction environment, which changes drastically due to the reaction rate [88]. Fig. 5 schematically shows how the concentration/source of protons and CO_2 and the pH vary as a function of the current density, indicating the current densities typically used in conventional lab-scale reactors (H-type), GDE-based flow reactors and industrial conditions.

This figure shows how the reactor, electrodes, and operative conditions can drastically change the availability of reactants at the surface and selectivity. Results at conventional lab-scale reactors may not be relevant for industrial operations because the micro-environment is different and, in turn, the optimal electrocatalysts. Most of the literature and reviews on CO_2RR focus on aspects such as intermediate binding energy, adsorbate–adsorbate interactions, defects sites, etc. These results are typically supported by theoretical studies, which do not account for the surface population, the presence and concentration of adsorbates, an interface with the electrolyte, and other crucial aspects. As also commented later, the behaviour in electrocatalysis is dominated instead by the concentration of species at the catalyst surface and interface with the electrolyte. Thus, mass transport phenomena and how they depend on the electrode and reactor design are crucial for parameters such as selectivity, onset potential and other aspects, which are typically ascribed to the intrinsic properties of the electrocatalyst.

The local environment directly influences reaction pathways and kinetics. Still, at the same time, the reaction modifies the local environment, depending on the balance between reaction and diffusion rates. The protons needed for the reduction of CO_2 derive, at very low current densities (<1 mA•cm^{-2}) and batch-type operations such as in H-type cells, mainly by hydronium ions present in the electrolyte. They can rapidly be depleted by increasing the current density. The process becomes conditioned by protons transported to the CO_2RR electrocatalysts and generated by water oxidation. When this process is not fast enough, the local pH increases. These pH changes would also affect the equilibria of CO_2-dissolved species, besides their transport rate. At moderate current densities in aqueous-fed systems (~30–60 mA•cm^{-2} but depending on the product), the CO_2 conversion rate depends on the diffusion limitations from the bulk electrolyte and the bicarbonate-hydrogen carbonate-carbonate ions equilibria [89]. These local environment changes ultimately impact key intermediates' surface coverage and binding energies on a catalyst's surface. These effects are further amplified at even higher current densities.

On the other hand, the choice of electrolyte and the characteristics of the GDE will strongly change the rate of these relative processes. Even inside GDE, the gradients could be relevant in determining a change in the local environment and electrocatalytic performances. Möller et al. [52] analysed the selectivity changes inside a GDE by modelling the overall mass transport variations within the porous catalytic layer of GDE in a cathodic current range of 50–700 mA•cm^{-2}. Their results are summarised in Fig. 6, which exemplifies the gradients present for high current density operations with a copper-based electrocatalyst.

The zone closest to the gas diffusion layer shows the highest concentration of CO_2 feed and the longest distance from the bulk $KHCO_3$ electrolyte. Thus, a region of high pH and CO_2 concentration favours the formation of C2 + products. Those conditions reverse progressively by moving to the outer part of the electrocatalyst layer, i.e. the one in direct contact with the electrolyte. Experimental evidence and simulations confirm this modelling [73,90–92]. These results suggest that the selectivity of CO_2RR is strongly influenced by the structure of the electrode and that electrode design has a fundamental role to optimize the effective gradients along the catalyst layer. In addition, the situation is expected to be quite different using a gas-phase GDE configuration due to the absence of the electrolyte, although still not analysed in the literature.

There are, in parallel, also changes in the spatial distribution of current density. Kas et al. [92], using a 2-D transport model, estimated the concentration gradients along the flow cell, the spatial distribution of the current density and the changes in local pH in the catalyst layer.

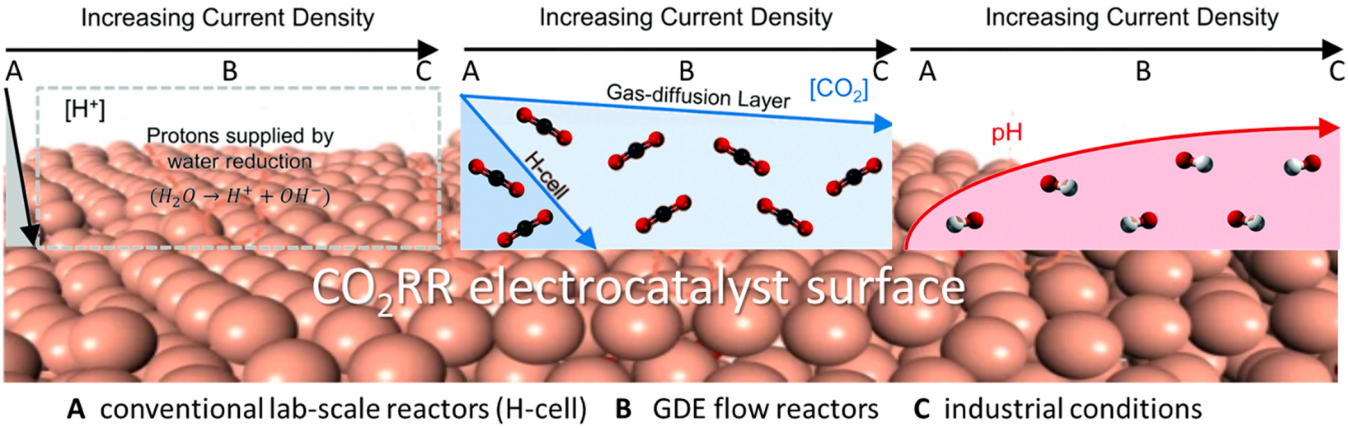

Fig. 5. Effect of current density on the availability of protons, concentration of CO_2 and pH at the surface of a CO_2RR electrocatalyst. Based on indications by Burdyny and Smith [88].

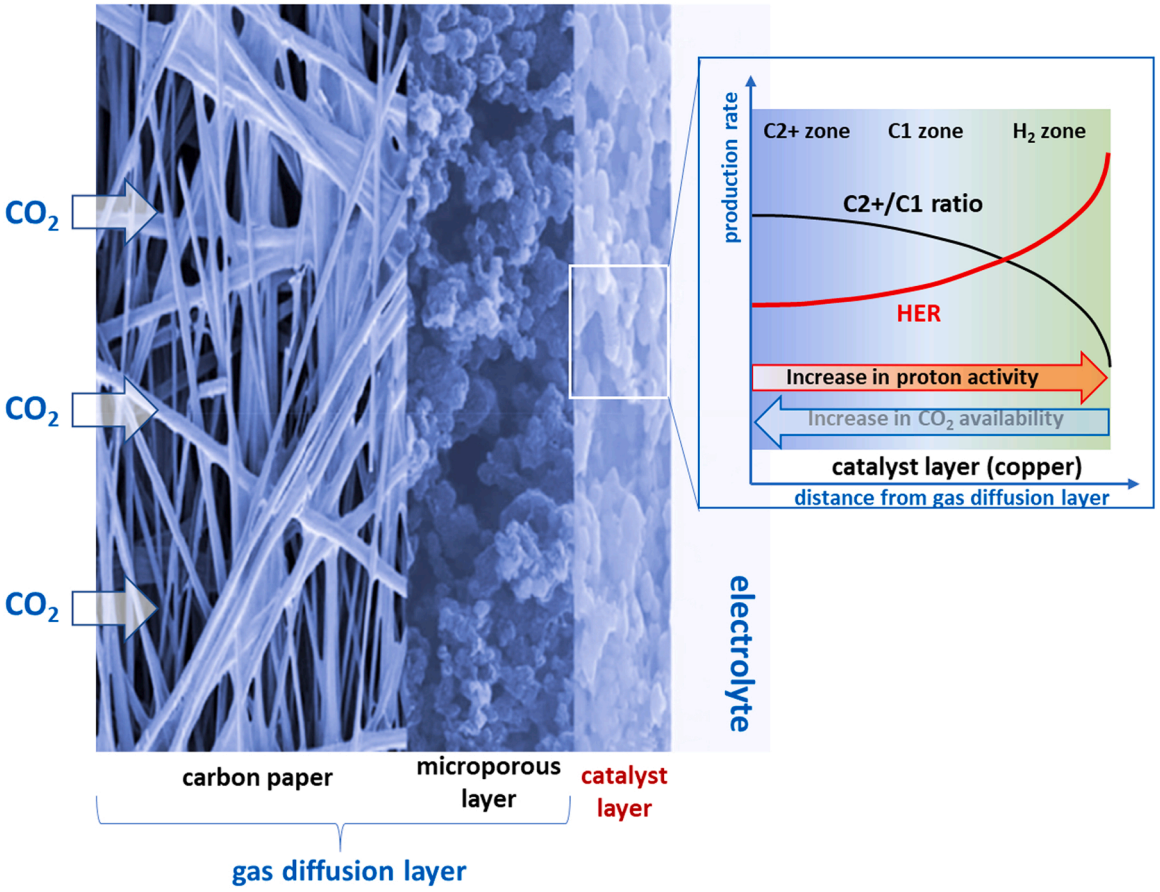

Fig. 6. Schematic cross-section of a GDE for CO_2RR operating at high current density. The expansion illustrates the concept of selectivity changing across the catalyst layer, with a zone where C2 + products are predominant, C1 products are predominant, and HER (hydrogen evolution reaction) is dominant. The zones are associated to variations in local pH (proton activity, red arrow) and local CO_2 concentration (CO_2 availability, blue arrow). Based on indications by Möller et al. [52,91].

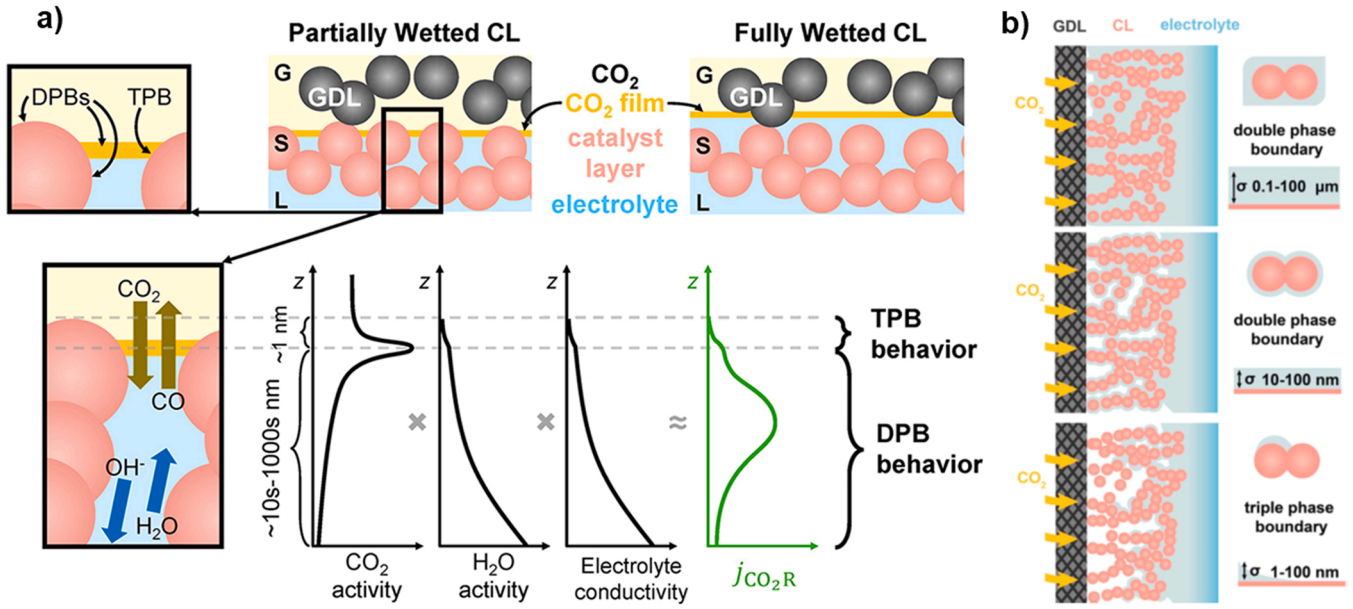

Fig. 7. (a) (top) Triple-phase and double-phase boundaries (TPB and DPB, respectively) in a GDE when the catalytic layer (CL) is partially or fully wetted. (bottom) Qualitative changes in CO_2 activity, H_2O activity, electrolyte conductivity, and the resulting CO_2RR current density. (b) Possible water arrangements in porous-metal CLs of CO_2RR GDEs in contact with an aqueous electrolyte and magnified images showing the thickness, σ, of the water layer between the gas and catalyst, with an indication of the formation of double- and triple-phase boundaries.
Adaptation with permission by Nesbitt et al. [41]. Copyright ACS, 2020.

At high single-pass conversions, they estimated significant concentration gradients along the flow channels leading to large local variations in the current density (>150 mA•cm^{-2}). These changes are prominent to ohmic losses. Furthermore, they estimated drastic changes in the concentration overpotentials with CO_2 flow rate.

Nesbitt et al. [41] reported similar concepts but introduced the presence of different phase boundaries along the GDE profile and related them to the wettability of the catalytic layer (CL), as illustrated in Fig. 7. Their calculation indicates that the reaction occurs primarily within 10–1000 nm of the gas-liquid interface, with the reactive thickness reducing to a few nanometers close to the interface for the highest current densities. The results indicate that to realise higher-current-density CO_2RR reactors, the CO_2 diffusion to the catalyst is crucial, thus realising a tailored mesoporosity in the CL. Flooding of the GDL will decrease CO_2 supply to the CL, with an optimal situation as illustrated in the middle part of Fig. 7b (a thin electrolyte film coating the catalysts NPs). In these conditions, the transport of protons and electrical conductivity become the critical factors rather than the diffusion of CO_2.

In the electrolyte-less GDE configuration, the diffusion of protons occurs mainly through surface diffusion from the membrane. The catalytic layer is prepared by spray drying an ink constituted by the catalytic nanoparticles over carbon support and additives to control hydrophobicity and ink characteristics. This solution is deposited on a GDL and then pressed to the proton-conductive membrane. There are thus analogies with the configuration presented in Fig. 7b for a thin electrolyte film coating the catalysts NPs.

Realising a three-phase interface to have an efficient electrocatalytic CO_2 reduction was indicated, among others, by Li et al. [42]. They suggest, however, the necessity of a design of a catalytic system that mimics the alveolus structure in mammalian lungs. This concept was realised by flexible, hydrophobic, nanoporous polyethylene membranes with high gas permeability and local alkalinity on the catalyst surface. These electrocatalysts show a FE of 92% (to CO), but low current densities (25.5 mA•cm^{-2}) at − 0.6 V versus RHE. However, based on the above discussion, this does not appear as the preferable solution to obtain high performances at high current densities.

Rabiee et al. [53] indicated the necessity of creating hydrophilic-hydrophobic layers (by in-situ electrooxidation) in the catalytic layer to maximise catalyst utilisation and triple-phase interfaces. This strategy was realised using a flow-through hollow fibre GDE coated with a Bi-embedded catalyst layer. The electrode having a tuned wettability showed over 80% catalyst utilisation and four times higher formate partial current density (about 150 mA•cm^{-2} with FE to formate over 90%) compared to the untreated electrode.

Li et al. [93] reviewed the role of electrode wettability in CO_2RR. They indicate that the electrodes' wettability strongly depends on the material chemistry, structures and electric field. Critical aspects include surface chemistry, electronic structures, dimensions, heterogeneity, microstructures, and modification by adding hydrophobic polymers, organic additives, and ionomers. The polarity, ionic nature, and ionic strengths of the liquid electrolytes also influence wettability. The electric field negatively impacts wettability because it enhances the solid-liquid interfacial interactions by re-distributing the charges at the interface. It plays a role in the electrochemical capillary pressure that drives the liquid motion in the solid pores and alters the local environment. Thus, many aspects influence this parameter, indicating the complex problems in describing the CO_2RR processes inside GDE. As emerged from the previous discussion, the description of the phenomena is still largely qualitative, notwithstanding the attempt to model them.

On the other hand, these results remark the need to design and engineer the electrode and the catalyst layer to balance the transport and reactions [45,63,88,93]. Realising optimal hydrophobic characteristics and electron distribution could fully utilise the electrochemical surface area, control the selectivity, and minimise flooding and ohmic losses [93]. Attempts in this direction have been reported in the literature, for example, to controlled addition of PTFE to optimise the wetting [42,89] or by treating the carbon black used as support for the catalyst by plasma treatment to introduce oxygen-containing groups and tune wettability [94].

The optimal positioning of the catalyst layer (CL) has to be identified by accounting for the possible electrolyte flooding and other phenomena commented on above. Thus, the optimal positioning of CL inside the GDE has to be identified considering all these factors and how they depend on the reactor and electride design.

The discussion up-to-now was centred on the flow-by-mode GDE design (e.g., the electrolyte flow tangential to the electrode [95]), which is the most obvious, but a flow-through mode is possible [64]. In this configuration, a high gas-to-liquid pressure drop can be maintained via pumping so that wettability becomes controlled by the liquid-wet surface [96–98]. Very interesting results have been obtained with this approach. For example, Lee et al. [98] used a zero-gap electrolyser (analogous to that indicated before as electrolyte-less, Fig. 8) to convert CO_2 to C_2H_4. Using Cu NPs modified by KOH (Cu-KOH) as an electrocatalyst on a GDL, they achieved a total current density of ~280 mA•cm^{-2} with ~55% FE_{C2H4} for an electrode with an area of 10 cm^2. The system is scalable from an industrial perspective.

3. Reactor configuration

The reactor configuration and design, as commented in the introduction, has a significant impact not only in terms of current density but all relevant parameters, including selectivity (Faradaic efficiency) and onset potential, which are instead typically ascribed to electrocatalyst characteristics. We do not claim the electrocatalyst itself is unimportant, but that the behaviour is dominated by electrode and reactor characteristics, determined mainly by transport phenomena and surface population by adspecies at the electrocatalyst surface. It is thus not unlikely that what is ascribed to different intrinsic characteristics of the electrocatalysts are instead related to other aspects, such as wettability, as discussed before, and their influence on the surface population by adspecies. Thus, methodologies that do not account for these aspects, including primarily the theoretical methods, fail to provide an accurate and reliable description of the effective aspects determining the electrocatalytic performances. We have not discussed the role of liquid electrolytes in this section because we consider that their use has to be overcome, as it will emerge from the following discussion. In addition, various reviews and papers have analyzed specifically the role of the electrolyte in CO_2RR [99–105].

Fig. 9 presents an overview of the main types of CO_2RR

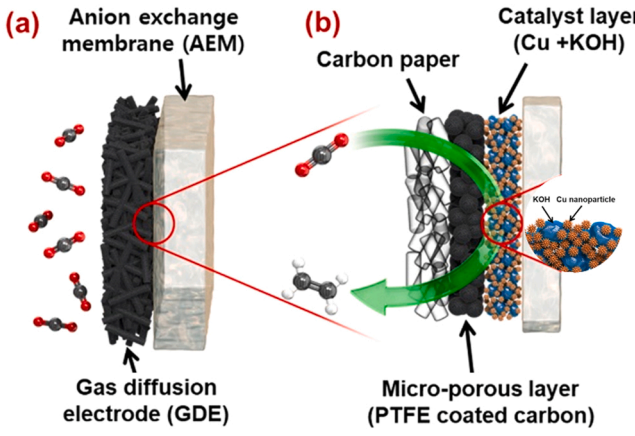

Fig. 8. KOH-incorporated Cu (Cu-KOH) electrodes in zero-gap electrolysers for CO_2RR to ethylene. (a) Schematic of assembled GDE and AEM in the zero-gap (electrolyte-less) configuration with an expansion of the GDE-AEM interface (b). Adaptation with permission by Lee et al. [98]. Copyright Elsevier, 2021.

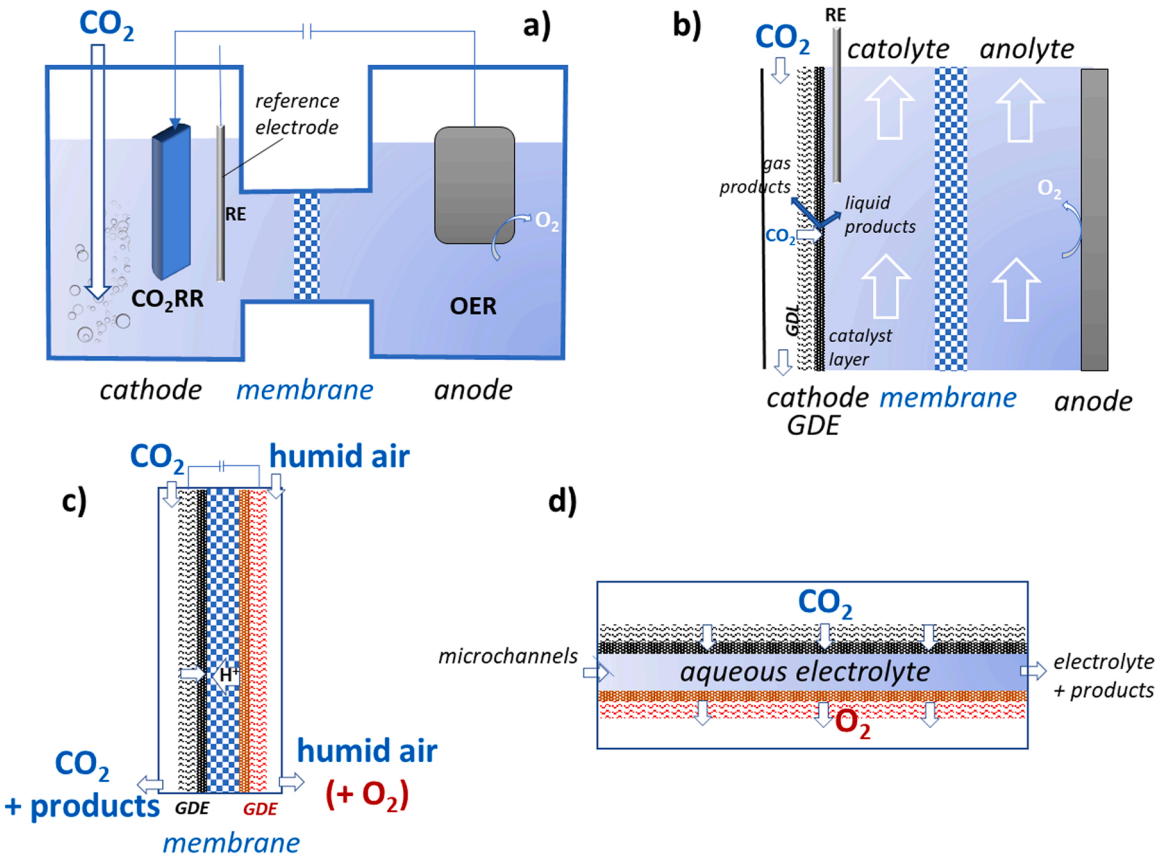

Fig. 9. Schematic diagram of CO_2RR electrolysers: (a) H-type cell; (b) GDE in a membrane-based flow cell; (c) advanced compact-design for zero-gap (electrolyte-less) flow cells with GDE on both anodic and cathodic sections; (d) microfluidic reactor.

electrocatalytic reactors. The most straightforward electrochemical device available for CO_2RR is a single-chamber cell. Three electrodes (working -WE-, counter -CE- and reference -RE- electrodes) are set in a single liquid environment. The working electrode is a bulk catalyst (e.g. a metal foil) or powder catalyst supported on a carbon substrate (carbon paper/cloth/fibres) or glassy carbon. The liquid is usually an aqueous solution of a salt (i.e. the electrolyte) pre-saturated with CO_2. During operations, CO_2 continuously flows into the system via a glass frit and then moves out to detect gas products. At the same time, liquid products are analysed off-line by sampling from the liquid electrolyte. At the anode, OER is typically used to balance the charge and close the electrical circuit. An ion-exchange membrane is normally used to divide the cell into two liquid compartments (with the option of operating with different catholyte and anolyte solutions). This is done to prevent the reduced and oxidized products from discharging onto the opposite electrodes (i.e. on the anode and cathode, respectively) and to close the electric circuit through ion transport and limit product crossover. The resulting cell is called an H-type cell due to its assumed shape resembling the letter H (see Fig. 9a). The electrocatalytic performances depend on the solubility of CO_2 in the electrolyte but are generally limited by the liquid electrolyte's slow mass transport.

The H-type cell is the most popular commercially available reactor used in the lab scale for the CO_2RR; most literature studies utilise this type of cell. Weekes et al. [50], in analysing papers published in the last decade (up to 2017) on metal-based electrocatalysts for CO_2RR, showed that only about 20 were made in a flow cell out of 1100 they analysed. Thus, H-cell experiments are largely dominating, even if the use of flow reactors is recently increasing. The H-type cells allow easier operations and adaptability to various electrodes. On the other hand, as commented before, they do not provide reliable indications of performances, especially at high current densities. Weekes et al. [50] remarked on using flow-type CO_2RR electrolysers because the information provided by H-type experiments is often not relevant to the dynamic environment of an electrolyzer [106,107]. In addition, mass transport in H-cell limits testing to current densities of < 100 mA•cm^{-2}, often even one order of magnitude lower. The electrocatalyst performances, and their selection, strongly depend on the current density. Thus, the results could give wrong indications even if used for an initial screening [88].

It was commented that CO_2RR energy efficiency is strongly negatively affected by the rapid and thermodynamically favourable reaction of CO_2 with hydroxide (OH^-) to form carbonate (CO_3^{2-}), which resulted in large voltage and CO_2 losses [108]. Rabinowitz and Kanan [108] indicate that hydroxide consumption makes alkaline CO_2 electrolyzers (as those commented before, which give the best performances in CO_2 to olefins [84–86]) fuel-wasting devices. High pH minimizes cell voltage due to chemical potential and the dependence of the thermodynamic electrode potentials on the pH. For this reason, it appears to have high energy efficiency.

However, the consumption of OH^- by CO_3^{2-} formation gives rise to a net negative energy balance. Fig. 10 helps to clarify this crucial issue. It reports thermodynamic cell potential (E°cell), cathode, anode, and BPM overpotentials (η). They are referenced to the standard hydrogen electrode (SHE). The green dotted line is the cathode potential reported by Ma et al. [109] for CO_2RR at > 200 mA•cm^{-2}. BPM indicates an electrocatalytic cell using a bipolar membrane, where CO_2 electrolysis is coupled with water dissociation at the BPM. Cell resistance was not included, which would add to the cell voltage. Alkaline conditions minimize cell voltage but cannot be maintained at a steady state because of CO_3^{2-} formation. The OH^- in the electrolyte reservoir is continuously consumed by exergonic CO_3^{2-} formation:

$$2OH^-_{(aq)} + CO_{2(g)} \rightarrow CO_{3(aq)}^{2-} + H_2O_{(l)}\ \Delta G^\circ = -56\ \text{kJ•mol}^{-1} \quad (1)$$

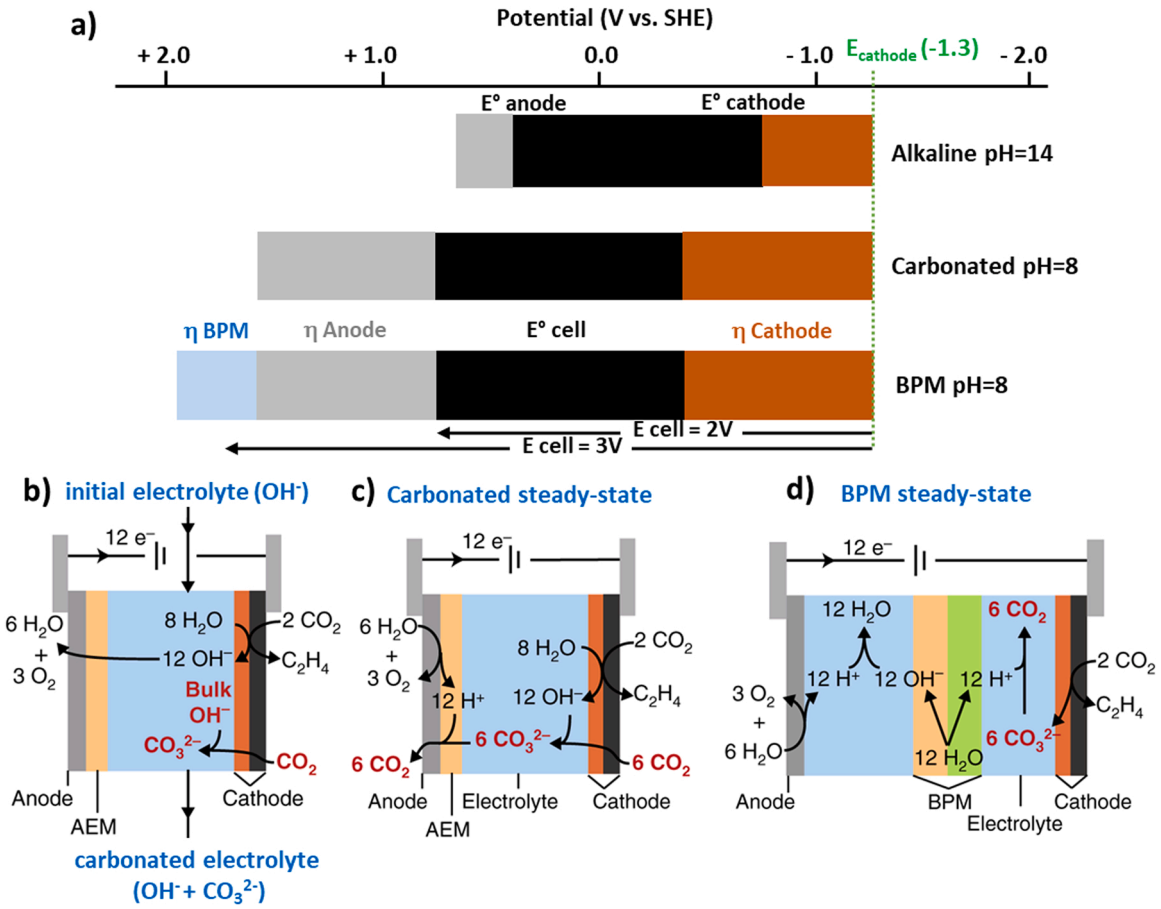

Fig. 10. (a) Contributors to the cell voltage for a CO_2RR electrolysis cell operating under alkaline conditions, carbonated conditions, or with a bipolar membrane (BPM). (b) Alkaline flow cell showing OH^- consumption by CO_2. (c) Cell at steady state after carbonation showing the carbon loss due to CO_2 released at the anode. (d) BPM cell at steady state.

The energy required to regenerate CO_2 and 2 OH^- from aqueous CO_3^{2-} is much larger than the energy stored by CO_2 electrolysis, with a negative energy balance of around ~100–130 kJ•mol^{-1} [108]. Besides putting a question mark on several published results operating in very strong alkaline conditions, such as those reported by various groups [84–86], Rabinowitz and Kanan [108] question whether, in general, it has a meaning to study CO_2RR. They conclude that avoiding the losses imposed by CO_3^{2-} formation demands creative cell designs. This objective could be realized by avoiding using a liquid electrolyte with a design like that presented in Fig. 9c. It is based on GDE at both the anode and cathode sides, with the membrane used as proton transfer and to close the ionic circuit. The other cell design also based on GDE, but still having a liquid electrolyte, as those presented in Figs. 9b and d, do not realize instead this objective.

Given the results presented in Fig. 10a, the use of a bipolar membrane (BPM) approach does not appear preferable, even if many studies in the literature have proposed this solution, mainly to obtain more stable performances and use different electrolytes on the two cells compartments [106,110,111]. BMPs promote the dissociation of H_2O into H^+ and OH^- by driving OH^- to the anode and H^+ to the cathode. They allow a constant pH on both sides of the cell, but these membranes increase the resistance and, thus, the potential required.

A microfluidic electrolyzer (Fig. 9d) does not use a membrane [112, 113]. The electrolyte flows in a microchannel (< 1 mm), with the crossover of reactants and products controlled by the laminar flow conditions. Two GDEs are used on the two sides of the channel. The reactor has a compact design and a high surface area to volume ratio, and there is a fast rate of CO_2 mass transfer to the cathode surface. However, product crossover is ineffective, and the construction/ management of the microfluidic electrolyzer is complex. It does not address the issues commented on before.

The zero-gap approach [43,45,98,114–117], also indicated earlier as electrolyte-less gas-phase operations or solid polymer electrolyte cells [45,50,55,56,118–123], seems the preferable reactor design from the state-of-the-art to obtain high performances and stability, coupled with cost-effective scalability. Since no RE is employed, the CO_2RR controls cell voltage or current rather than WE potential. Endrődi et al. [117] reported CO_2 reduction to CO with a partial current density of 420 mA•cm^{-2} stable for over 200 h, demonstrating the scalability on a multicell electrolyser stack, with an active area of 100 cm^2 per cell. However, the cathode must be periodically infused with alkali cation-containing solutions to avoid precipitate formation. Lee et al. [98] reported an FE to ethylene in CO_2RR of 50% at a current density of 200 mA•cm^{-2}. De Mot et al. [124] reported the possibility of obtaining high formate concentration from CO_2RR (up to 60 g L^{-1} at 100 mA•cm^{-2}) using a method of direct water injection on a catholyte-free zero-gap CO_2 electrolyzer. Alinejad et al. [125] showed how the performance of the same catalyst could be substantially different in a zero-gap / GDE approach to H-cell measurements, confirming the comments made above. Gabardo et al. [126] reported ~50% and ~80% FE to ethylene and C2 + products (the other main product is ethanol), respectively, in CO_2RR using zero-gap electrolyzers with stability for over 100 h continuous operation at current densities > 100 mA•cm^{-2}. Larrazábal et al. [127] used this zero-gap approach to convert electrocatalytically CO_2 to CO with partial current density up to ca. 200 mA•cm^{-2} with minimal H_2 production. Fan et al. [128] used this

zero-gap approach (although called all-solid-state reactor) for CO_2RR to formate, obtaining a formate partial current densities ~450 mA•cm^{-2}, FE up to ~97% and high stability (100 h) on a grain boundary-enriched bismuth electrocatalyst.

Lee et al. [129] indicated that this approach is the preferable strategy to reduce the capital cost of electrolyzers. Gawel et al. [130] also suggest that this reactor approach is preferable to improve economics. Park et al. [131] indicate this solution is preferable towards large-scale CO_2RR.

Thus, many converging indications are remarking how this zero-gap (or electrolyte-less, gas-phase, or solid polymer electrolyte cells) is the preferable electrode/reactor strategy in implementing CO_2RR from an industrial perspective, although many challenges still remain, among them, controlling the precipitation of carbonates at high current densities [132] and designing specific, high-performance membranes [133].

4. EIS studies

Understanding more precisely the controlling resistances and mass transfer phenomena in zero-gap electrolysers, their difference with respect to performances in the presence of an electrolyzer and how these aspects could influence the selectivity are critical aspects emerging from the previous discussion. It is necessary to use methods providing in situ indications but sensitive to the above aspects, including those concerning the reactor design. Electrochemical impedance spectroscopy (EIS) combined with cyclic voltammetry (CV) is a suitable methodology for this scope and was recently applied by Giusi et al. [51]. While other authors used EIS as a primary diagnostic tool to understand CO_2RR [134–136], Giusi et al. [51] were the first to use the method to understand the differences between the presence or absence of a liquid electrolyte, linking the selectivity (in particular to C2 + products) to the differences in surface transport properties related to the presence or not of the liquid electrolyte.

EIS is a valuable technique for investigating the charge transfer and transport processes involved in electrocatalytic processes. Still, it is also an excellent in situ diagnostic tool to determine changes in the electrocatalytic properties due to deactivation, for example, in industrial electrocatalytic reactors [137]. EIS is based on the application of a sinusoidal voltage V with variable frequency to the system under study and on the measure of the current response to this perturbation. EIS data are typically fitted through an equivalent electrical circuit composed of elements (resistances, capacitances, etc.) mimicking the electrical behaviour of the system under study. The fitting gives quantitative information about the processes involved in the reaction.

In CO_2RR, the method provides useful mechanistic indications about the processes controlling the reactivity. Bienen et al. [135,136] identified in EIS curves of a GDE electrode (tin-based electrocatalysts supported on carbon; for CO_2RR to formate and CO) four main features (Fig. 11): (i) ionic and electronic conductivity in the porous system, (ii) the reaction of CO_2 with OH^- to form bicarbonate, (iii) charge transfer converting CO_2 (aq) to $CO_2^{\bullet-}$, and (iv) liquid phase diffusion of CO_2 (aq). The shape-dominating reaction switches with varying temperatures, CO_2 volume fraction, current density, and electrolytes. The method provides thus excellent information on the dominant processes depending on the electrode characteristics and operative conditions. Fig. 12.

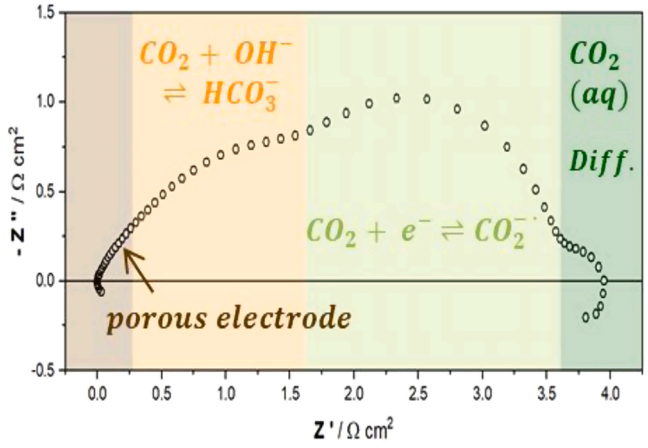

Fig. 11. Different processes determining the EIS curves in CO_2RR using a GDE electrode (aqueous 1.0 M KOH as the electrolyte). Tin-based electrocatalysts supported on carbon for CO_2RR to formate and CO.
Reproduced with permission by Bienen et al. [136]. Copyright ACS, 2020.

Giusi et al. [51] used EIS, together with CV and electrocatalytic tests, to investigate copper-based (Cu_xO) GDE in a zero-gap electrocatalytic reactor, comparing the results with analogous tests, but in the presence of a liquid electrolyte (aqueous $KHCO_3$). The same electrocatalyst gives different products in CO_2RR. C2 + products essentially do not form in the presence of the liquid electrolyte, except for minor amounts of oxalic acid at the lower voltages. On the contrary, various C2 products, particularly ethanol at the higher voltage, acetaldehyde, acetic acid and even C3 products such as isopropanol, were formed in electrolyte-less conditions (thus zero-gap electrode). Formic acid, the primary product at the higher voltages in the presence of the liquid electrolyte, was not detected in its absence. Therefore, a drastic change in product distribution was observed.

EIS and CV results explain the difference, which can be summarized as follows:

1. presence liquid electrolyte → i) proton reduction is dominant, and ii) protons compete with CO_2 intermediate species in the adsorption;
2. without the liquid electrolyte → the local concentration of CO_2 on the electrode surface is higher than CO_2 in liquid-phase operations because proton supplying becomes the limiting step.

The drastic change in the catalytic behaviour (C2 + products detected only in gas-phase operations) is thus related to how the electrode and reactor operative conditions determine the population of the surface species at the electrocatalyst surface and, in turn, the paths of transformation, rather than the intrinsic catalyst properties.

Cyclic voltammetry (CV) also results evidence a change in the in situ reconstruction of the electrocatalyst depending on the applied potential. In electrolyte-less tests, the nanostructure of the copper NPs changes from packed nanocubes to nanorod shape with a diameter of about 200 nm and length of around 5–15 μm. This in situ reconstruction occurs at a potential more negative than about − 1.0 V, leading to an enhanced current density. This reconstruction did not occur in the presence of the liquid electrolyte, evidencing further relevant aspects of the dynamic of the surface electrocatalytic processes and how significant reconstruction processes may occur in situ when the potential is applied. Still, they depend on the presence or not of the electrolyte.

5. Industrial scalability

In general, to drive the CO_2RR process in an economically feasible way for industrial scalability, the electrodes/devices should operate: i) at a high current density to provide a high conversion rate; ii) at low cell voltage to enhance energy efficiency; and iii) with high Faradaic Efficiency, to increase the selectivity to value-added products (e.g. C2 +). Many parameters should be optimized according to the reactor configuration adopted to achieve these conditions suitable for industrial applicability.

As discussed above, the CO_2RR process can be realized in different devices, but not all these configurations can be successfully adopted for scaling-up operations. Table 1 reports a qualitative comparison of some selected parameters indicating the performance of the four types of electrochemical cells reported in Fig. 9.

Excluding the H-type cell, which is typically used in the early stage of

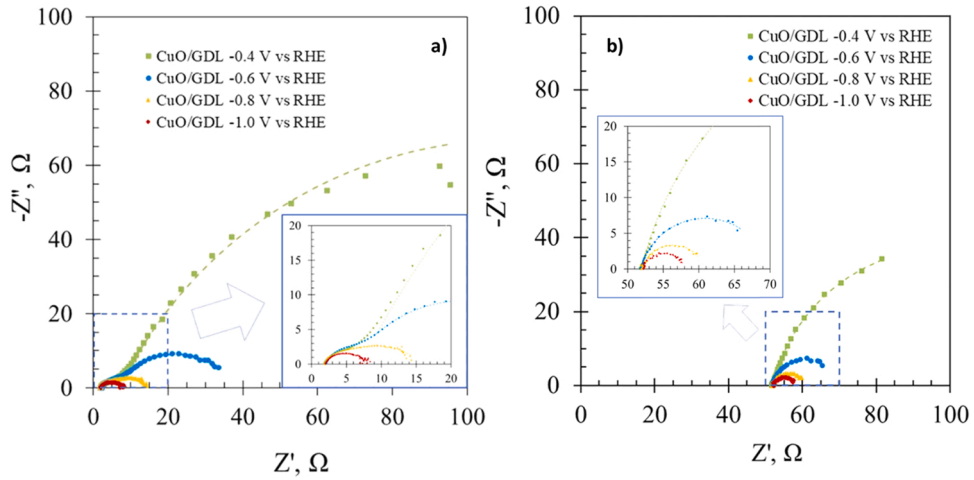

Fig. 12. Nyquist plots for CuO/GDL electrode at different applied potentials obtained in a liquid electrolyte device saturated with CO_2 (a) and without the electrolyte, in a zero-gap GDE electrode (b). Copyright Elsevier, 2022.
Adapted with permission by Giusi et al. [51].

Table 1
Comparison for different process parameters and performance indicators of the four types of electrochemical cells reported in Fig. 9. (■: good; ▼: bad; –: medium).

	H-type cell	*Flow-by cell (GDE in a membrane-based flow cell)*	*Zero-gap (flow cells (electrolyte-less)*	*Microfluidic reactor*
Pressure drop	■	–	■	–
Current density	▼	–	■	■
Uniform distribution of current	▼	–	■	–
Gas handling	▼	■	■	–
Complex design	■	–	▼	▼[145,160]

laboratory screening of catalysts/electrodes, the zero-gap (electrolyte-less) option is the most promising reactor configuration for obtaining high current density under industrial scale. A zero-gap GDE electrolyser can be manufactured in a stackable configuration, operate with high current density with minimal ohmic resistance, and be designed for a mass production application [89]. One of the options recently investigated for zero-gap configuration is using multiple electrolyze layers with a pressurized CO_2 gas feed (up to 10 bar), which is a common practice in PEM water electrolyser, but rarely used for CO_2RR [96]. This electrolyser allows a uniform distribution of CO_2 gas among the layers and operates identically to the sum of multiple single-layer electrolyser cells but with increased CO_2 conversion efficiency. Implementing this concept can accelerate technology development to scale up electrochemical CO_2RR to an industrially relevant level.

Table 2
General reaction conditions for CO_2RR operations in zero-gap configuration, including the operating conditions, electrode surface area, current density, cell voltage, the power required to run the system and gas feed.

Operating conditions	Temperature = 20–100 °C, Pressure = 0–30 bar
Electrode surface area	0.1–100 cm^2
Current density	100–500 mA cm^{-2}
Cell voltage	2–5 V
Energy Efficiency	20–45%
Power (energy required to run the system)	0.1–10 W (per cm^2 of electrode surface area)
Gas feed	Usually, humidified pure CO_2 stream

With a focus on zero-gap GDE electrolyzers for the motivations indicated above, Table 2 summarizes typical reaction conditions for CO_2RR operations, including the operating conditions, electrode surface area, current density, cell voltage, the power required to run the system and gas feed.

Table 3 instead reports selected literature indications on the main reaction conditions for CO_2RR operations in zero-gap configuration, including the current density, Faradaic Efficiency, electrode surface area and gas feed. These two tables provide a general summary to help readers develop advanced zero-gap-type electrolyzers.

The general major drawback of zero-gap GDE configuration is the system's complexity, mainly due to the realization of a membrane electrode assembly with a high-surface area.

Salt precipitation is another general issue for industrial scalability in CO_2RR electrolyser, as it may cause flooding and hinder gas transport, thus limiting long-term durability. Salt precipitation is regularly observed in zero-gap GDE configurations, especially in operations at high current densities. However, many engineering strategies have recently been developed for preventing or reserving salt formation in zero-gap systems [138]. These approaches include: i) modifying the anolyte concentration and composition, ii) adding solvents to the cathode, iii) pulsed electrolysis, and iv) reconversion of (bi)carbonate back to CO_2 using a bipolar membrane.

Furthermore, other important process parameters, such as the cell temperature, the humidification of CO_2, and the cell compression, should be carefully investigated for achieving industrial-relevant CO_2RR activities [139].

Industrial-relevant current densities with high FE and energy efficiency can only be achieved by moving beyond today's research from catalyst development to an integrated electrode and reactor design, which allows the exploitation of the viable potential of CO_2RR catalysts.

The viability of CO_2RR commercialization is also influenced by the reaction occurring at the anode, usually the oxygen evolution reaction (OER). As O_2 has a limited value, different anodic reactions should be performed in an industrial reactor to achieve a higher economic impact.

Once the CO_2RR technologies reach industrial applicability, they may treat all kinds of gaseous waste streams coming from many processes, i.e. from chemical or biochemical process industries.

A viable emergent application of CO_2RR is integrating biochemical processes as an alternative industrial route for food production [140]. CO_2, CO and H_2 can be upgraded to fuels and chemicals through gas-phase fermentation by selected bacteria, although with low volumetric efficiency due to gas-liquid mass transfer limitations. The electrocatalytic conversion of CO_2 to more soluble products (i.e. acetate)

Table 3
Main reaction conditions for CO_2RR operations in zero-gap configuration, including the current density, Faradaic Efficiency, electrode surface area and gas feed, from selected literature.

	Current density, $mA \cdot cm^{-2}$	*Main products*	*Faradaic Efficiency (FE), %*	*Potential*	*Electrode surface area, cm^2*	*Gas feed*	*Reference*
KOH-incorporated Cu nanoparticle	281	C2, ethylene	C2 products: 78.7% (54.5% to C_2H_4)	Cell voltage = 3.0–3.5 V	10	humidified CO_2 (99.999%) at 80 °C and 1 M KOH solution	Lee et al.[98]
$[Ni(Cyc)]^{2+}$ (Cyc = cyclam = 1,4,8,11-tetraazacyclotetradecane) and $[Ni(CycCOOH)]^{2+}$ (CycCOOH = 1,4,8,11-tetraazacyclotetradecane-6-carboxylic acid)	100	CO	> 30%	Cell voltage = 3.7–3.9 V	5	humidified CO_2 at 20 sccm	Siritanaratkul et al.[114]
Ag nanoparticles	420	CO	90	Cell voltage = 3.2 V	8 (demonstrated scalability to 100 cm^2)	humidified CO_2	Endrődi et al. [117]
Au colloidal NPs	> 200	CO	~40 (until 60% at lower current density)	− 1.0 V versus RHE	0.07	humidified CO_2 stream (16 mL min^{-1})	Alinejad et al. [125]
Ag nanocubes	> 300	CO	85	− 1.8 V versus Ag/AgCl	0.07	humidified CO_2 stream (16 mL min−1)	Gálvez-Vázquez et al.[132]
Ag nanoparticles	300	CO	30 (until 45% at lower humidity)	Cell voltage = 3.0 V	2	CO_2 (50 mL min^{-1}) + Argon (5.5 mL min^{-1}) stream	Hoof et al.[139]

opens the route towards forming carbon substrates that a broad range of organisms can metabolize and thus allow food production independent of biological photosynthesis.

6. Conclusions, perspectives and recommendations

This viewpoint has discussed the role of the electrode and reactor design in CO_2RR. The results evidence the need to pass to zero-gap (e.g., electrolyte-less) reactors, based on GDE electrode design, to obtain more reliable results, especially from the perspective of industrialization. However, as remarked, their use should not be sequential after the experiments in batch-type reactors or even simpler flow-type electrocatalytic reactors. Many parameters characterizing the performances, such as Faradaic efficiency, carbon selectivity and potential onset, besides the current density, are strongly influenced and typically dominated by the effective population of adspecies on the electrocatalyst surface than from the catalyst's intrinsic properties.

Even the preliminary screening of the catalysts may be incorrect without operating under representative conditions, and thus by making a proper choice of the electrode and reactor. At the same time, these indications also evidence that most of the literature design criteria, based on studies that do not account for the effective population of adspecies on the electrocatalyst surface, such as theoretical methods, largely fail to reproduce the effective critical factors determining the catalyst choice and design. We have indicated some of the crucial aspects in catalyst design, such as wettability, which are typically not included in the factors determining the paths of CO_2RR.

The methods to investigate the electrocatalysts and electrode should be selected to provide information on aspects such as i) the diffusion of protons and CO_2 species, ii) the resistances which are present and how they depend on the operative conditions and type of electrode, iii) the phase-boundary generated, and iv) the effective operando electrocatalyst surface. Electrochemical characterization methods like EIS, CV and CA are necessary to study electrocatalytic reactions. Still, other techniques should complement them, particularly operando methods such as ambient pressure X-ray photoelectron spectroscopy (APXPS) and near-edge X-ray absorption fine structure spectroscopy (NEXAFS) [36,72]. These advanced surface-sensitive in situ spectroscopic methods are very useful to understand better the nature of the active interphase and its dynamic dependence on the experimental conditions during CO_2RR. In these operando conditions, significant reconstructions of the active species' nature may also occur, depending on the applied potential and the type of electrode and other operative conditions, including the presence or absence of a liquid electrolyte. Research attention is increasing, as various reviews indicate [141–145].

The challenge of enabling the industrialization of CO_2RR processes thus requires going beyond several current approaches and studies and obtaining a better understanding of the phenomena and design aspects discussed in this viewpoint. While there is increasing attention on these design and engineering aspects (from macro to nanoscale), as commented in this paper, still most of the attention in the literature is instead dedicated to discussing the nature of the electrocatalyst, with a large emphasis on a contribution by theoretical modelling, as the primary relevant strategy for CO_2RR [146–156], with aspects on mass transport, electrode and reactor engineering, fluido dynamics, etc. as eventually an additional level to consider. We indicated in this viewpoint that it is instead necessary to turn the vision on the electrode and reactor design as the main factor determining the performances, at least under reaction conditions relevant to industrial scalability. While we do not neglect that aspects such as modulating the electronic structure, adsorption geometries and the local environment of the catalysts could determine the CO_2RR performance under some specific testing conditions, these factors often become largely not pertinent under relevant conditions of testing. In contrast, other aspects determine the behaviour and, in turn, the design of the "optimal" system.

As a final comment and recommendation, it must be clarified that most of the literature studies on CO_2RR have limited attention on the application of the technology, which must avoid a series of critical constraints, from the need to use pure CO_2 feed to expensive designs of the electrode and reactors. It is necessary to include solutions to these critical issues already at the technology's development stage because they significantly determine the performance and results. Once the CO_2RR technologies reach industrial applicability, they may be used to treat gaseous waste streams from many processes, i.e., chemical or biochemical process industries.

In addition to advanced emerging solutions for various applications, from energy-intensive industries to distributed production of energy vectors or chemicals [13,14,157], visionary possibilities exist, such as the mentioned possibility of producing food (proteins) from the air. Many other "dream" possibilities exist, from producing fertilizers from the air to artificial tree devices for hydrogen production with integrated storage [158]. Thus, electrocatalysis is crucial in meeting

decarbonization challenges [159]. It has to address many challenges [160–163]. Still, it can become an enabling technology when the current attention mainly focused on the electrocatalyst is broadened, taking into better consideration the role of electrode/reactor design and the crucial aspects from an industrial perspective.

CRediT authorship contribution statement

Claudio Ampelli: Performed Writing – original draft, Conceptualization, Supervision. **Gabriele Centi:** Performed Writing – original draft, Conceptualization, Supervision. All the other authors contributed to the Investigation, Methodology, Resources, and Validation.

Declaration of Competing Interest

The authors declare the following financial interests/personal relationships which may be considered as potential competing interests: S Perathoner reports financial support was provided by Italian Ministry of University and Research. G Centi reports financial support was provided by European Commission. GC also thanks the Alexander von Humboldt-Stiftung/Foundation (Humboldt Research Award).

Data Availability

No data was used for the research described in the article.

Acknowledgements

The European Union funded this work through the DECADE H2020 project (ID: 862030) and by the MIUR (Italy) through the PRIN Project CO_2 ONLY (No. 2017WR2LRS), which are gratefully acknowledged. GC also thanks the Alexander von Humboldt-Stiftung/Foundation (Humboldt Research Award).

References

[1] G. Centi, S. Perathoner, Catalysis for an electrified chemical production, Catal. Today, Press (2022), 10.1016/j.cattod.2022.10.017 (2022).
[2] C. Ampelli, S. Perathoner, G. Centi, CO_2 utilization: an enabling element to move to a resource- and energy-efficient chemical and fuel production, philosophical transactions of the Royal Society A: mathematical, Phys. Eng. Sci. 373 (2015) 20140177.
[3] P. Lanzafame, S. Abate, C. Ampelli, C. Genovese, R. Passalacqua, G. Centi, S. Perathoner, Beyond solar fuels: renewable energy-driven chemistry, ChemSusChem 10 (2017) 4409–4419.
[4] W. Zhang, Z. Jin, Z. Chen, Rational-designed principles for electrochemical and photoelectrochemical upgrading of CO_2 to value-added chemicals, Adv. Sci. 9 (2022) 2105204.
[5] P. Saha, S. Amanullah, A. Dey, Selectivity in electrochemical CO_2 reduction, Acc. Chem. Res. 55 (2022) 134–144.
[6] W. Ma, X. He, W. Wang, S. Xie, Q. Zhang, Y. Wang, Electrocatalytic reduction of CO_2 and CO to multi-carbon compounds over Cu-based catalysts, Chem. Soc. Rev. 50 (2021) 12897–12914.
[7] G. Wang, J. Chen, Y. Ding, P. Cai, L. Yi, Y. Li, C. Tu, Y. Hou, Z. Wen, L. Dai, Electrocatalysis for CO_2 conversion: from fundamentals to value-added products, Chem. Soc. Rev. 50 (2021) 4993–5061.
[8] X. Tan, C. Yu, Y. Ren, S. Cui, W. Li, J. Qiu, Recent advances in innovative strategies for the CO_2 electroreduction reaction, Energy Environ. Sci. 14 (2021) 765–780.
[9] G. Centi, S. Perathoner, Chapter 1 - turning CO_2 into fuels and chemicals: an introduction, chemical valorisation of carbon dioxide, R. Soc. Chem. (2023) 1–18.
[10] G. Centi, S. Perathoner, The chemical engineering aspects of CO_2 capture, combined with its utilisation, Curr. Opin. Chem. Eng. 39 (2023), 100879.
[11] S. Perathoner, G. Centi, Catalysis for solar-driven chemistry: the role of electrocatalysis, Catal. Today 330 (2019) 157–170.
[12] G. Centi, S. Perathoner, Catalytic technologies for the conversion and reuse of CO_2, in: M. Lackner, B. Sajjadi, W.-Y. Chen (Eds.), Handbook of Climate Change Mitigation and Adaptation, Springer International Publishing, Cham, 2022, pp. 1803–1852.
[13] S. Perathoner, K.M. Van Geem, G.B. Marin, G. Centi, Reuse of CO_2 in energy intensive process industries, Chem. Commun. 57 (2021) 10967–10982.
[14] A. Appolloni, G. Centi, N. Yang, Promoting carbon circularity for a sustainable and resilience fashion industry, Curr. Opin. Green. Sustain. Chem. 39 (2023), 100719.
[15] K.M. Van Geem, B.M. Weckhuysen, Toward an e-chemistree: materials for electrification of the chemical industry, MRS Bull. 46 (2021) 1187–1196.
[16] G. Papanikolaou, G. Centi, S. Perathoner, P. Lanzafame, Catalysis for e-chemistry: need and gaps for a future de-fossilized chemical production, with focus on the role of complex (direct) syntheses by electrocatalysis, ACS Catal. 12 (2022) 2861–2876.
[17] G. Centi, S. Perathoner, Status and gaps toward fossil-free sustainable chemical production, Green. Chem. 24 (2022) 7305–7331.
[18] B. Kumar, J.P. Brian, V. Atla, S. Kumari, K.A. Bertram, R.T. White, J.M. Spurgeon, New trends in the development of heterogeneous catalysts for electrochemical CO_2 reduction, Catal. Today 270 (2016) 19–30.
[19] Z. Masood, Q. Ge, Electrochemical reduction of CO_2 at the earth-abundant transition metal-oxides/copper interfaces, Catal. Today 409 (2023) 53–62.
[20] I.E.L. Stephens, K. Chan, A. Bagger, S.W. Boettcher, J. Bonin, E. Boutin, A. K. Buckley, R. Buonsanti, E.R. Cave, X. Chang, S.W. Chee, A.H.M. da Silva, P. de Luna, O. Einsle, B. Endrődi, M. Escudero-Escribano, J.V. Ferreira de Araujo, M. C. Figueiredo, C. Hahn, K.U. Hansen, S. Haussener, S. Hunegnaw, Z. Huo, Y. J. Hwang, C. Janáky, B.S. Jayathilake, F. Jiao, Z.P. Jovanov, P. Karimi, M.T. M. Koper, K.P. Kuhl, W.H. Lee, Z. Liang, X. Liu, S. Ma, M. Ma, H.-S. Oh, M. Robert, B.R. Cuenya, J. Rossmeisl, C. Roy, M.P. Ryan, E.H. Sargent, P. Sebastián-Pascual, B. Seger, L. Steier, P. Strasser, A.S. Varela, R.E. Vos, X. Wang, B. Xu, H. Yadegari, Y. Zhou, roadmap on low temperature electrochemical CO_2 reduction, J. Phys. Energy 4 (2022) (2022), 042003.
[21] S. Nitopi, E. Bertheussen, S.B. Scott, X. Liu, A.K. Engstfeld, S. Horch, B. Seger, I.E. L. Stephens, K. Chan, C. Hahn, J.K. Nørskov, T.F. Jaramillo, I. Chorkendorff, Progress and perspectives of electrochemical CO_2 reduction on copper in aqueous electrolyte, Chem. Rev. 119 (2019) 7610–7672.
[22] F. Dattila, R.R. Seemakurthi, Y. Zhou, N. López, Modeling operando electrochemical CO_2 reduction, Chem. Rev. 122 (2022) 11085–11130.
[23] T.-D. Nguyen-Phan, L. Hu, B.H. Howard, W. Xu, E. Stavitski, D. Leshchev, A. Rothenberger, K.C. Neyerlin, D.R. Kauffman, High current density electroreduction of CO_2 into formate with tin oxide nanospheres, Sci. Rep. 12 (2022) 8420.
[24] K.C. Poon, W.Y. Wan, H. Su, H. Sato, A review on recent advances in the electrochemical reduction of CO_2 to CO with nano-electrocatalysts, RSC Adv. 12 (2022) 22703–22721.
[25] F. Chang, M. Xiao, R. Miao, Y. Liu, M. Ren, Z. Jia, D. Han, Y. Yuan, Z. Bai, L. Yang, Copper-based catalysts for electrochemical carbon dioxide reduction to multicarbon products, Electrochem. Energy Rev. 5 (2022) 4.
[26] J. Li, A. Xu, F. Li, Z. Wang, C. Zou, C.M. Gabardo, Y. Wang, A. Ozden, Y. Xu, D.-H. Nam, Y. Lum, J. Wicks, B. Chen, Z. Wang, J. Chen, Y. Wen, T. Zhuang, M. Luo, X. Du, T.-K. Sham, B. Zhang, E.H. Sargent, D. Sinton, Enhanced multi-carbon alcohol electroproduction from CO via modulated hydrogen adsorption, Nat. Commun. 11 (2020) 3685.
[27] X. Wang, Z. Wang, F.P. García de Arquer, C.-T. Dinh, A. Ozden, Y.C. Li, D.-H. Nam, J. Li, Y.-S. Liu, J. Wicks, Z. Chen, M. Chi, B. Chen, Y. Wang, J. Tam, J. Y. Howe, A. Proppe, P. Todorović, F. Li, T.-T. Zhuang, C.M. Gabardo, A. R. Kirmani, C. McCallum, S.-F. Hung, Y. Lum, M. Luo, Y. Min, A. Xu, C.P. O'Brien, B. Stephen, B. Sun, A.H. Ip, L.J. Richter, S.O. Kelley, D. Sinton, E.H. Sargent, Efficient electrically powered CO_2-to-ethanol via suppression of deoxygenation, Nat. Energy 5 (2020) 478–486.
[28] J. Li, F. Che, Y. Pang, C. Zou, J.Y. Howe, T. Burdyny, J.P. Edwards, Y. Wang, F. Li, Z. Wang, P. De Luna, C.-T. Dinh, T.-T. Zhuang, M.I. Saidaminov, S. Cheng, T. Wu, Y.Z. Finfrock, L. Ma, S.-H. Hsieh, Y.-S. Liu, G.A. Botton, W.-F. Pong, X. Du, J. Guo, T.-K. Sham, E.H. Sargent, D. Sinton, Copper adparticle enabled selective electrosynthesis of n-propanol, Nature, Communications 9 (2018) 4614.
[29] J.H. Montoya, A.A. Peterson, J.K. Nørskov, Insights into C-C coupling in CO_2 electroreduction on copper electrodes, ChemCatChem 5 (2013) 737–742.
[30] J.D. Goodpaster, A.T. Bell, M. Head-Gordon, Identification of possible pathways for C–C bond formation during electrochemical reduction of CO_2: new theoretical insights from an improved electrochemical model, J. Phys. Chem. Lett. 7 (2016) 1471–1477.
[31] T. Möller, F. Scholten, T.N. Thanh, I. Sinev, J. Timoshenko, X. Wang, Z. Jovanov, M. Gliech, B. Roldan Cuenya, A.S. Varela, P. Strasser, Electrocatalytic CO_2 reduction on CuO_x nanocubes: tracking the evolution of chemical state, geometric structure, and catalytic selectivity using operando spectroscopy, Angew. Chem. Int. Ed. 59 (2020) 17974–17983.
[32] X. Zhang, S.-X. Guo, K.A. Gandionco, A.M. Bond, J. Zhang, Electrocatalytic carbon dioxide reduction: from fundamental principles to catalyst design, Mater. Today Adv. 7 (2020), 100074.
[33] A.R. Akbashev, Electrocatalysis on oxide surfaces: fundamental challenges and opportunities, Curr. Opin. Electrochem. 35 (2022), 101095.
[34] Y.Y. Birdja, E. Pérez-Gallent, M.C. Figueiredo, A.J. Göttle, F. Calle-Vallejo, M.T. M. Koper, Advances and challenges in understanding the electrocatalytic conversion of carbon dioxide to fuels, Nat. Energy 4 (2019) 732–745.
[35] J. Linnemann, K. Kanokkanchana, K. Tschulik, Design strategies for electrocatalysts from an electrochemist's perspective, ACS Catal. 11 (2021) 5318–5346.
[36] R. Arrigo, R. Blume, V. Streibel, C. Genovese, A. Roldan, M.E. Schuster, C. Ampelli, S. Perathoner, J.J. Velasco Vélez, M. Hävecker, A. Knop-Gericke, R. Schlögl, G. Centi, Dynamics at polarized carbon dioxide–iron oxyhydroxide interfaces unveil the origin of multicarbon product formation, ACS Catal. 12 (2022) 411–430.
[37] A. Senocrate, C. Battaglia, Electrochemical CO_2 reduction at room temperature: Status and perspectives, J. Energy Storage 36 (2021), 102373.

[38] Y. Chen, D. Su, Y. Chen, Z. Zhu, W. Li, Three-phase interface-assisted advanced electrochemistry-related applications, Cell Rep. Phys. Sci. 2 (2021), 100602.
[39] D. Wakerley, S. Lamaison, F. Ozanam, N. Menguy, D. Mercier, P. Marcus, M. Fontecave, V. Mougel, Bio-inspired hydrophobicity promotes CO_2 reduction on a Cu surface, Nat. Mater. 18 (2019) 1222–1227.
[40] M. Melchionna, P. Fornasiero, M. Prato, M. Bonchio, Electrocatalytic CO_2 reduction: role of the cross-talk at nano-carbon interfaces, Energy Environ. Sci. 14 (2021) 5816–5833.
[41] N.T. Nesbitt, T. Burdyny, H. Simonson, D. Salvatore, D. Bohra, R. Kas, W. A. Smith, Liquid–solid boundaries dominate activity of CO_2 reduction on gas-diffusion electrodes, ACS Catal. 10 (2020) 14093–14106.
[42] J. Li, G. Chen, Y. Zhu, Z. Liang, A. Pei, C.-L. Wu, H. Wang, H.R. Lee, K. Liu, S. Chu, Y. Cui, Efficient electrocatalytic CO_2 reduction on a three-phase interface, Nat. Catal. 1 (2018) 592–600.
[43] Y. Yang, F. Li, Reactor design for electrochemical CO_2 conversion toward large-scale applications, Curr. Opin. Green. Sustain. Chem. 27 (2021), 100419.
[44] P. Jeanty, C. Scherer, E. Magori, K. Wiesner-Fleischer, O. Hinrichsen, M. Fleischer, Upscaling and continuous operation of electrochemical CO_2 to CO conversion in aqueous solutions on silver gas diffusion electrodes, J. CO_2 Util. 24 (2018) 454–462.
[45] J.-B. Vennekoetter, R. Sengpiel, M. Wessling, Beyond the catalyst: how electrode and reactor design determine the product spectrum during electrochemical CO_2 reduction, Chem. Eng. J. 364 (2019) 89–101.
[46] S.S. Bhargava, F. Proietto, D. Azmoodeh, E.R. Cofell, D.A. Henckel, S. Verma, C. J. Brooks, A.A. Gewirth, P.J.A. Kenis, System design rules for intensifying the electrochemical reduction of CO_2 to CO on Ag nanoparticles, ChemElectroChem 7 (2020) 2001–2011.
[47] D. Xu, K. Li, B. Jia, W. Sun, W. Zhang, X. Liu, T. Ma, Electrocatalytic CO_2 reduction towards industrial applications, Carbon Energy 5 (2023), e230.
[48] R. Lin, J. Guo, X. Li, P. Patel, A. Seifitokaldani, Electrochemical reactors for CO_2 conversion, Catalysts (2020).
[49] B.C. Marepally, C. Ampelli, C. Genovese, T. Saboo, S. Perathoner, F.M. Wisser, L. Veyre, J. Canivet, E.A. Quadrelli, G. Centi, Enhanced formation of >C1 products in electroreduction of CO_2 by adding a CO_2 adsorption component to a gas-diffusion layer-type catalytic electrode, ChemSusChem 10 (2017) 4442–4446.
[50] D.M. Weekes, D.A. Salvatore, A. Reyes, A. Huang, C.P. Berlinguette, Electrolytic CO_2 Reduction in a Flow Cell, Acc. Chem. Res. 51 (2018) 910–918.
[51] D. Giusi, M. Miceli, C. Genovese, G. Centi, S. Perathoner, C. Ampelli, In situ electrochemical characterization of Cu_xO-based gas-diffusion electrodes (GDEs) for CO_2 electrocatalytic reduction in presence and absence of liquid electrolyte and relationship with C2+ products formation, Appl. Catal. B: Environ. 318 (2022), 121845.
[52] T. Möller, T. Ngo Thanh, X. Wang, W. Ju, Z. Jovanov, P. Strasser, The product selectivity zones in gas diffusion electrodes during the electrocatalytic reduction of CO_2, Energy Environ. Sci. 14 (2021) 5995–6006.
[53] H. Rabiee, L. Ge, J. Zhao, X. Zhang, M. Li, S. Hu, S. Smart, T.E. Rufford, Z. Zhu, H. Wang, Z. Yuan, Regulating the reaction zone of electrochemical CO_2 reduction on gas-diffusion electrodes by distinctive hydrophilic-hydrophobic catalyst layers, Appl. Catal. B: Environ. 310 (2022), 121362.
[54] B. Pan, Y. Wang, Y. Li, Understanding and leveraging the effect of cations in the electrical double layer for electrochemical CO_2 reduction, Chem. Catal. 2 (2022) 1267–1276.
[55] C. Ampelli, G. Centi, R. Passalacqua, S. Perathoner, Electrolyte-less design of PEC cells for solar fuels: prospects and open issues in the development of cells and related catalytic electrodes, Catal. Today 259 (2016) 246–258.
[56] S. Perathoner, G. Centi, D. Su, Turning perspective in photoelectrocatalytic cells for solar fuels, ChemSusChem 9 (2016) 345–357.
[57] K. Ehelebe, N. Schmitt, G. Sievers, A.W. Jensen, A. Hrnjić, P. Collantes Jiménez, P. Kaiser, M. Geuß, Y.-P. Ku, P. Jovanovič, K.J.J. Mayrhofer, B. Etzold, N. Hodnik, M. Escudero-Escribano, M. Arenz, S. Cherevko, Benchmarking fuel cell electrocatalysts using gas diffusion electrodes: inter-lab comparison and best practices, ACS Energy Lett. 7 (2022) 816–826.
[58] S. Fransen, S. Ballet, J. Fransaer, S. Kuhn, Overcoming diffusion limitations in electrochemical microreactors using acoustic streaming, J. Flow. Chem. 10 (2020) 307–325.
[59] J. Wang, C.-X. Zhao, J.-N. Liu, D. Ren, B.-Q. Li, J.-Q. Huang, Q. Zhang, Quantitative kinetic analysis on oxygen reduction reaction: a perspective, Nano Mater. Sci. 3 (2021) 313–318.
[60] S.T. Dix, S. Lu, S. Linic, Critical practices in rigorously assessing the inherent activity of nanoparticle electrocatalysts, ACS Catal. 10 (2020) 10735–10741.
[61] J.M. Doña Rodríguez, J.A. Herrera Melián, J. Pérez Peña, Determination of the real surface area of Pt electrodes by hydrogen adsorption Using Cyclic Voltammetry, J. Chem. Educ. 77 (2000) 1195.
[62] M. Gangeri, G. Centi, A.L. Malfa, S. Perathoner, R. Vieira, C. Pham-Huu, M. J. Ledoux, Electrocatalytic performances of nanostructured platinum–carbon materials, Catal. Today, 102- 103 (2005) 50–57.
[63] S. Garg, M. Li, A.Z. Weber, L. Ge, L. Li, V. Rudolph, G. Wang, T.E. Rufford, Advances and challenges in electrochemical CO_2 reduction processes: an engineering and design perspective looking beyond new catalyst materials, J. Mater. Chem. A 8 (2020) 1511–1544.
[64] V. Vedharathinam, Z. Qi, C. Horwood, B. Bourcier, M. Stadermann, J. Biener, M. Biener, Using a 3D porous flow-through electrode geometry for high-rate electrochemical reduction of CO_2 to CO in ionic liquid, ACS Catal. 9 (2019) 10605–10611.
[65] S.R. Hui, N. Shaigan, V. Neburchilov, L. Zhang, K. Malek, M. Eikerling, P. Luna, Three-dimensional cathodes for electrochemical reduction of CO_2: from macro- to nano-engineering, Nanomaterials 10 (2020) 1884.
[66] E. Vaněčková, M. Bouša, V. Shestivska, J. Kubišta, P. Moreno-García, P. Broekmann, M. Rahaman, M. Zlámal, J. Heyda, M. Bernauer, T. Sebechlebská, V. Kolivoška, Electrochemical reduction of carbon dioxide on 3D printed electrodes, ChemElectroChem 8 (2021) 2137–2149.
[67] J. Lai, A. Nsabimana, R. Luque, G. Xu, 3D Porous carbonaceous electrodes for electrocatalytic applications, Joule 2 (2018) 76–93.
[68] F.C. Walsh, L.F. Arenas, C. Ponce de León, Developments in electrode design: structure, decoration and applications of electrodes for electrochemical technology, J. Chem. Technol. Biotechnol. 93 (2018) 3073–3090.
[69] A.Z. Weber, R.L. Borup, R.M. Darling, P.K. Das, T.J. Dursch, W. Gu, D. Harvey, A. Kusoglu, S. Litster, M.M. Mench, R. Mukundan, J.P. Owejan, J.G. Pharoah, M. Secanell, I.V. Zenyuk, A critical review of modeling transport phenomena in polymer-electrolyte fuel cells, J. Electrochem. Soc. 161 (2014) F1254.
[70] F. Li, D.R. MacFarlane, J. Zhang, Recent advances in the nanoengineering of electrocatalysts for CO_2 reduction, Nanoscale 10 (2018) 6235–6260.
[71] J.-J. Velasco-Vélez, T. Jones, D. Gao, E. Carbonio, R. Arrigo, C.-J. Hsu, Y.-C. Huang, C.-L. Dong, J.-M. Chen, J.-F. Lee, P. Strasser, B. Roldan Cuenya, R. Schlögl, A. Knop-Gericke, C.-H. Chuang, The role of the copper oxidation state in the electrocatalytic reduction of CO_2 into valuable hydrocarbons, ACS Sustain. Chem. Eng. 7 (2019) 1485–1492.
[72] C. Genovese, M.E. Schuster, E.K. Gibson, D. Gianolio, V. Posligua, R. Grau-Crespo, G. Cibin, P.P. Wells, D. Garai, V. Solokha, S. Krick Calderon, J.J. Velasco-Velez, C. Ampelli, S. Perathoner, G. Held, G. Centi, R. Arrigo, Operando spectroscopy study of the carbon dioxide electro-reduction by iron species on nitrogen-doped carbon, Nat. Commun. 9 (2018) 935.
[73] L.-C. Weng, A.T. Bell, A.Z. Weber, Modeling gas-diffusion electrodes for CO_2 reduction, Phys. Chem. Chem. Phys. 20 (2018) 16973–16984.
[74] A. Fernández-Barquín, C. Casado-Coterillo, M. Palomino, S. Valencia, A. Irabien, Permselectivity improvement in membranes for CO_2/N_2 separation, Sep. Purif. Technol. 157 (2016) 102–111.
[75] X. Chen, K.G. Khoo, M.W. Kim, L. Hong, Deriving a CO_2-permselective carbon membrane from a multilayered matrix of polyion complexes, ACS Appl. Mater. Interfaces 6 (2014) 10220–10230.
[76] S. Fujikawa, R. Selyanchyn, T. Kunitake, A new strategy for membrane-based direct air capture, Polym. J. 53 (2021) 111–119.
[77] J.F. de Brito, C. Genovese, F. Tavella, C. Ampelli, M.V. Boldrin Zanoni, G. Centi, S. Perathoner, CO_2 reduction of hybrid Cu_2O–Cu/Gas diffusion layer electrodes and their integration in a Cu-based photoelectrocatalytic cell, ChemSusChem 12 (2019) 4274–4284.
[78] J.F. de Brito, F. Tavella, C. Genovese, C. Ampelli, M.V.B. Zanoni, G. Centi, S. Perathoner, Role of CuO in the modification of the photocatalytic water splitting behavior of TiO_2 nanotube thin films, Appl. Catal. B: Environ. 224 (2018) 136–145.
[79] J.A.L. Perini, F. Tavella, E.P. Ferreira Neto, M.V.B. Zanoni, S.J.L. Ribeiro, D. Giusi, G. Centi, S. Perathoner, C. Ampelli, Role of nanostructure in the behaviour of $BiVO_4$–TiO_2 nanotube photoanodes for solar water splitting in relation to operational conditions, Sol. Energy Mater. Sol. Cells 223 (2021), 110980.
[80] M. Li, E. Irtem, H.-P. Iglesias van Montfort, M. Abdinejad, T. Burdyny, Energy comparison of sequential and integrated CO_2 capture and electrochemical conversion, Nat. Commun. 13 (2022) 5398.
[81] M. Jouny, W. Luc, F. Jiao, General techno-economic analysis of CO_2 electrolysis systems, Ind. Eng. Chem. Res. 57 (2018) 2165–2177.
[82] S. Verma, B. Kim, H.-R.M. Jhong, S. Ma, P.J.A. Kenis, A. Gross-Margin, Model for defining technoeconomic benchmarks in the electroreduction of CO_2, ChemSusChem 9 (2016) 1972–1979.
[83] J.M. Spurgeon, B. Kumar, A comparative technoeconomic analysis of pathways for commercial electrochemical CO_2 reduction to liquid products, Energy Environ. Sci. 11 (2018) 1536–1551.
[84] M. Ma, E.L. Clark, K.T. Therkildsen, S. Dalsgaard, I. Chorkendorff, B. Seger, Insights into the carbon balance for CO_2 electroreduction on Cu using gas diffusion electrode reactor designs, Energy Environ. Sci. 13 (2020) 977–985.
[85] G.L. De Gregorio, T. Burdyny, A. Loiudice, P. Iyengar, W.A. Smith, R. Buonsanti, Facet-dependent selectivity of Cu catalysts in electrochemical CO_2 reduction at commercially viable current densities, ACS Catal. 10 (2020) 4854–4862.
[86] C.-T. Dinh, T. Burdyny, M.G. Kibria, A. Seifitokaldani, C.M. Gabardo, F.P. García de Arquer, A. Kiani, J.P. Edwards, P. De Luna, O.S. Bushuyev, C. Zou, R. Quintero-Bermudez, Y. Pang, D. Sinton, E.H. Sargent, CO_2 electroreduction to ethylene via hydroxide-mediated copper catalysis at an abrupt interface, Science 360 (2018) 783–787.
[87] R. Kas, K. Yang, D. Bohra, R. Kortlever, T. Burdyny, W.A. Smith, Electrochemical CO_2 reduction on nanostructured metal electrodes: fact or defect? Chem. Sci. 11 (2020) 1738–1749.
[88] T. Burdyny, W.A. Smith, CO_2 reduction on gas-diffusion electrodes and why catalytic performance must be assessed at commercially-relevant conditions, Energy Environ. Sci. 12 (2019) 1442–1453.
[89] M.R. Singh, E.L. Clark, A.T. Bell, Effects of electrolyte, catalyst, and membrane composition and operating conditions on the performance of solar-driven electrochemical reduction of carbon dioxide, Phys. Chem. Chem. Phys. 17 (2015) 18924–18936.
[90] S. Suter, S. Haussener, Optimizing mesostructured silver catalysts for selective carbon dioxide conversion into fuels, Energy Environ. Sci. 12 (2019) 1668–1678.

[91] L.-C. Weng, A.T. Bell, A.Z. Weber, A systematic analysis of Cu-based membrane-electrode assemblies for CO_2 reduction through multiphysics simulation, Energy Environ. Sci. 13 (2020) 3592–3606.

[92] R. Kas, A.G. Star, K. Yang, T. Van Cleve, K.C. Neyerlin, W.A. Smith, Along the channel gradients impact on the spatioactivity of gas diffusion electrodes at high conversions during CO_2 electroreduction, ACS Sustain. Chem. Eng. 9 (2021) 1286–1296.

[93] M. Li, M.N. Idros, Y. Wu, T. Burdyny, S. Garg, X.S. Zhao, G. Wang, T.E. Rufford, The role of electrode wettability in electrochemical reduction of carbon dioxide, J. Mater. Chem. A 9 (2021) 19369–19409.

[94] R. Shi, J. Guo, X. Zhang, G.I.N. Waterhouse, Z. Han, Y. Zhao, L. Shang, C. Zhou, L. Jiang, T. Zhang, Efficient wettability-controlled electroreduction of CO_2 to CO at Au/C interfaces, Nat. Commun. 11 (2020) 3028.

[95] E.M. Remillard, A.N. Shocron, J. Rahill, M.E. Suss, C.D. Vecitis, A direct comparison of flow-by and flow-through capacitive deionization, Desalination 444 (2018) 169–177.

[96] B. Endrődi, E. Kecsenovity, A. Samu, F. Darvas, R.V. Jones, V. Török, A. Danyi, C. Janáky, Multilayer electrolyzer stack converts carbon dioxide to gas products at high pressure with high efficiency, ACS Energy Lett. 4 (2019) 1770–1777.

[97] Z. Gu, H. Shen, Z. Chen, Y. Yang, C. Yang, Y. Ji, Y. Wang, C. Zhu, J. Liu, J. Li, T.-K. Sham, X. Xu, G. Zheng, Efficient electrocatalytic CO_2 reduction to C2+ alcohols at defect-site-rich Cu surface, Joule 5 (2021) 429–440.

[98] W.H. Lee, C. Lim, S.Y. Lee, K.H. Chae, C.H. Choi, U. Lee, B.K. Min, Y.J. Hwang, H.-S. Oh, Highly selective and stackable electrode design for gaseous CO_2 electroreduction to ethylene in a zero-gap configuration, Nano Energy 84 (2021), 105859.

[99] P. Sebastián-Pascual, S. Mezzavilla, I.E.L. Stephens, M. Escudero-Escribano, Structure-sensitivity and electrolyte effects in CO_2 electroreduction: from model studies to applications, ChemCatChem 11 (2019) 3626–3645.

[100] R.M. Arán-Ais, D. Gao, B. Roldan Cuenya, Structure- and electrolyte-sensitivity in CO_2 electroreduction, Acc. Chem. Res. 51 (2018) 2906–2917.

[101] G. Marcandalli, M.C.O. Monteiro, A. Goyal, M.T.M. Koper, Electrolyte effects on CO_2 electrochemical reduction to CO, Acc. Chem. Res. 55 (2022) 1900–1911.

[102] T. Li, C. Yang, J.-L. Luo, G. Zheng, Electrolyte driven highly selective CO_2 electroreduction at low overpotentials, ACS Catal. 9 (2019) 10440–10447.

[103] M. Moura de Salles Pupo, R. Kortlever, Electrolyte effects on the electrochemical reduction of CO_2, ChemPhysChem 20 (2019) 2926–2935.

[104] M. König, J. Vaes, E. Klemm, D. Pant, Solvents and supporting electrolytes in the electrocatalytic reduction of CO_2, iScience 19 (2019) 135–160.

[105] R.J. Gomes, C. Birch, M.M. Cencer, C. Li, S.-B. Son, I.D. Bloom, R.S. Assary, C. V. Amanchukwu, Probing electrolyte influence on CO_2 reduction in aprotic solvents, J. Phys. Chem. C. 126 (2022) 13595–13606.

[106] Y.C. Li, D. Zhou, Z. Yan, R.H. Gonçalves, D.A. Salvatore, C.P. Berlinguette, T. E. Mallouk, Electrolysis of CO_2 to syngas in bipolar membrane-based electrochemical cells, ACS Energy Lett. 1 (2016) 1149–1153.

[107] B. Endrődi, G. Bencsik, F. Darvas, R. Jones, K. Rajeshwar, C. Janáky, Continuous-flow electroreduction of carbon dioxide, Prog. Energy Combust. Sci. 62 (2017) 133–154.

[108] J.A. Rabinowitz, M.W. Kanan, The future of low-temperature carbon dioxide electrolysis depends on solving one basic problem, Nat. Commun. 11 (2020) 5231.

[109] W. Ma, S. Xie, T. Liu, Q. Fan, J. Ye, F. Sun, Z. Jiang, Q. Zhang, J. Cheng, Y. Wang, Electrocatalytic reduction of CO_2 to ethylene and ethanol through hydrogen-assisted C–C coupling over fluorine-modified copper, Nat. Catal. 3 (2020) 478–487.

[110] J. Balster, D.F. Stamatialis, M. Wessling, Electro-catalytic membrane reactors and the development of bipolar membrane technology, Chem. Eng. Process.: Process. Intensif. 43 (2004) 1115–1127.

[111] N.M. Vargas-Barbosa, G.M. Geise, M.A. Hickner, T.E. Mallouk, Assessing the utility of bipolar membranes for use in photoelectrochemical water-splitting cells, ChemSusChem 7 (2014) 3017–3020.

[112] R.S. Jayashree, S.K. Yoon, F.R. Brushett, P.O. Lopez-Montesinos, D. Natarajan, L. J. Markoski, P.J.A. Kenis, On the performance of membraneless laminar flow-based fuel cells, J. Power Sources 195 (2010) 3569–3578.

[113] D.T. Whipple, E.C. Finke, P.J.A. Kenis, Microfluidic reactor for the electrochemical reduction of carbon dioxide: the effect of pH, Electrochem. Solid-State Lett. 13 (2010) B109.

[114] B. Siritanaratkul, M. Forster, F. Greenwell, P.K. Sharma, E.H. Yu, A.J. Cowan, Zero-gap bipolar membrane electrolyzer for carbon dioxide reduction using acid-tolerant molecular electrocatalysts, J. Am. Chem. Soc. 144 (2022) 7551–7556.

[115] Y. Nishimura, D. Yoshida, M. Mizuhata, K. Asaka, K. Oguro, H. Takenaka, Solid polymer electrolyte CO_2 reduction, Energy Convers. Manag. 36 (1995) 629–632.

[116] M. Sassenburg, M. Kelly, S. Subramanian, W.A. Smith, T. Burdyny, Zero-gap electrochemical CO_2 reduction cells: challenges and operational strategies for prevention of salt precipitation, ACS Energy Lett. (2022) 321–331.

[117] B. Endrődi, A. Samu, E. Kecsenovity, T. Halmágyi, D. Sebők, C. Janáky, Operando cathode activation with alkali metal cations for high current density operation of water-fed zero-gap carbon dioxide electrolysers, Nat. Energy 6 (2021) 439–448.

[118] C. Ampelli, G. Centi, R. Passalacqua, S. Perathoner, Synthesis of solar fuels by a novel photoelectrocatalytic approach, Energy Environ. Sci. 3 (2010) 292–301.

[119] C. Ampelli, C. Genovese, B.C. Marepally, G. Papanikolaou, S. Perathoner, G. Centi, Electrocatalytic conversion of CO_2 to produce solar fuels in electrolyte or electrolyte-less configurations of PEC cells, Faraday Discuss. 183 (2015) 125–145.

[120] I. Merino-Garcia, E. Alvarez-Guerra, J. Albo, A. Irabien, Electrochemical membrane reactors for the utilisation of carbon dioxide, Chem. Eng. J. 305 (2016) 104–120.

[121] R.L. Cook, R.C. MacDuff, A.F. Sammells, Ambient temperature gas phase CO_2 reduction to hydrocarbons at solid polymer electrolyte cells, J. Electrochem. Soc. 135 (1988) 1470.

[122] L.M. Aeshala, R. Uppaluri, A. Verma, Electrochemical conversion of CO_2 to fuels: tuning of the reaction zone using suitable functional groups in a solid polymer electrolyte, Phys. Chem. Chem. Phys. 16 (2014) 17588–17594.

[123] N. Gutiérrez-Guerra, L. Moreno-López, J.C. Serrano-Ruiz, J.L. Valverde, A. de Lucas-Consuegra, Gas phase electrocatalytic conversion of CO_2 to syn-fuels on Cu based catalysts-electrodes, Appl. Catal. B: Environ. 188 (2016) 272–282.

[124] B. De Mot, M. Ramdin, J. Hereijgers, T.J.H. Vlugt, T. Breugelmans, Direct water injection in catholyte-free zero-gap carbon dioxide electrolyzers, ChemElectroChem 7 (2020) 3839–3843.

[125] S. Alinejad, J. Quinson, G.K.H. Wiberg, N. Schlegel, D. Zhang, Y. Li, S. Reichenberger, S. Barcikowski, M. Arenz, Electrochemical reduction of CO_2 on Au electrocatalysts in a zero-gap, half-cell gas diffusion electrode setup: a systematic performance evaluation and comparison to an H-cell setup, ChemElectroChem 9 (2022), e202200341.

[126] C.M. Gabardo, C.P. O'Brien, J.P. Edwards, C. McCallum, Y. Xu, C.T. Dinh, J. Li, E. H. Sargent, D. Sinton, Continuous carbon dioxide electroreduction to concentrated multi-carbon products using a membrane electrode assembly, Joule 3 (2019) 2777–2791.

[127] G.O. Larrazábal, P. Strøm-Hansen, J.P. Heli, K. Zeiter, K.T. Therkildsen, I. Chorkendorff, B. Seger, Analysis of mass flows and membrane cross-over in CO_2 reduction at high current densities in an MEA-type electrolyzer, ACS Appl. Mater. Interfaces 11 (2019) 41281–41288.

[128] L. Fan, C. Xia, P. Zhu, Y. Lu, H. Wang, Electrochemical CO_2 reduction to high-concentration pure formic acid solutions in an all-solid-state reactor, Nature, Communications 11 (2020) 3633.

[129] W.H. Lee, K. Kim, C. Lim, Y.-J. Ko, Y.J. Hwang, B.K. Min, U. Lee, H.-S. Oh, New strategies for economically feasible CO_2 electroreduction using a porous membrane in zero-gap configuration, J. Mater. Chem. A 9 (2021) 16169–16177.

[130] A. Gawel, T. Jaster, D. Siegmund, J. Holzmann, H. Lohmann, E. Klemm, U.-P. Apfel, Electrochemical CO_2 reduction - the macroscopic world of electrode design, reactor concepts & economic aspects, iScience 25 (2022), 104011.

[131] S. Park, D.T. Wijaya, J. Na, C.W. Lee, Towards the large-scale electrochemical reduction of carbon dioxide, Catalysts 11 (2021) 253.

[132] M. de Jesus Gálvez-Vázquez, P. Moreno-García, H. Xu, Y. Hou, H. Hu, I. Z. Montiel, A.V. Rudnev, S. Alinejad, V. Grozovski, B.J. Wiley, M. Arenz, P. Broekmann, Environment matters: CO_2RR electrocatalyst performance testing in a gas-fed zero-gap electrolyzer, ACS Catal. 10 (2020) 13096–13108.

[133] D.A. Salvatore, C.M. Gabardo, A. Reyes, C.P. O'Brien, S. Holdcroft, P. Pintauro, B. Bahar, M. Hickner, C. Bae, D. Sinton, E.H. Sargent, C.P. Berlinguette, Designing anion exchange membranes for CO_2 electrolysers, Nat. Energy 6 (2021) 339–348.

[134] A. Sacco, Electrochemical impedance spectroscopy as a tool to investigate the electroreduction of carbon dioxide: a short review, J. CO_2 Util. 27 (2018) 22–31.

[135] F. Bienen, D. Kopljar, S. Geiger, N. Wagner, K.A. Friedrich, Investigation of CO_2 electrolysis on tin foil by electrochemical impedance spectroscopy, ACS Sustain. Chem. Eng. 8 (2020) 5192–5199.

[136] F. Bienen, D. Kopljar, A. Löwe, S. Geiger, N. Wagner, E. Klemm, K.A. Friedrich, Revealing mechanistic processes in gas-diffusion electrodes during CO_2 reduction via impedance spectroscopy, ACS Sustain. Chem. Eng. 8 (2020) 13759–13768.

[137] A. Sanginario, S. Hernández, Diagnostics of electrocatalytic systems by electrochemical impedance spectroscopy, Curr. Opin. Green. Sustain. Chem. 39 (2023), 100727.

[138] M. Sassenburg, M. Kelly, S. Subramanian, W.A. Smith, T. Burdyny, Zero-gap electrochemical CO_2 reduction cells: challenges and operational strategies for prevention of salt precipitation, ACS Energy Lett. 8 (2023) 321–331.

[139] L. Hoof, N. Thissen, K. Pellumbi, K. junge Puring, D. Siegmund, A.K. Mechler, U.-P. Apfel, Hidden parameters for electrochemical carbon dioxide reduction in zero-gap electrolyzers, cell reports physical, Science 3 (2022), 100825.

[140] E.C. Hann, S. Overa, M. Harland-Dunaway, A.F. Narvaez, D.N. Le, M.L. Orozco-Cárdenas, F. Jiao, R.E. Jinkerson, A hybrid inorganic–biological artificial photosynthesis system for energy-efficient food production, Nat. Food 3 (2022) 461–471.

[141] Y. Yang, Y. Xiong, R. Zeng, X. Lu, M. Krumov, X. Huang, W. Xu, H. Wang, F. J. DiSalvo, J.D. Brock, D.A. Muller, H.D. Abruña, Operando methods in electrocatalysis, ACS Catal. 11 (2021) 1136–1178.

[142] C. Long, J. Han, J. Guo, C. Yang, S. Liu, Z. Tang, Operando toolbox for heterogeneous interface in electrocatalysis, Chem. Catal. 1 (2021) 509–522.

[143] J. Timoshenko, B. Roldan Cuenya, In situ/operando electrocatalyst characterization by X-ray absorption spectroscopy, Chem. Rev. 121 (2021) 882–961.

[144] R. Arrigo, In situ X-ray spectroscopic characterization techniques for electrocatalysis, Curr. Opin. Green. Sustain. Chem. 34 (2022), 100601.

[145] L. Jin, A. Seifitokaldani, In situ spectroscopic methods for electrocatalytic CO_2 reduction, Catalysts 10 (2020) 481.

[146] B. Seger, M. Robert, F. Jiao, Best practices for electrochemical reduction of carbon dioxide, Nat. Sustain. (2023).

[147] J. Zhu, S. Das, P. Cool, Chapter Two - Recent strategies for the electrochemical reduction of CO_2 into methanol, in: M. Diéguez, A.W. Kleij (Eds.), Advances in Catalysis, Academic Press, 2022, pp. 29–62.

[148] S. Sarkar, S.C. Peter, Catalyst designing strategies for electrochemical CO_2 reduction: a perspective, Prog. Energy 4 (2022), 032002.

[149] W. Choi, D.H. Won, Y.J. Hwang, Catalyst design strategies for stable electrochemical CO_2 reduction reaction, J. Mater. Chem. A 8 (2020) 15341–15357.

[150] W. Lai, Y. Qiao, J. Zhang, Z. Lin, H. Huang, Design strategies for markedly enhancing energy efficiency in the electrocatalytic CO_2 reduction reaction, Energy Environ. Sci. 15 (2022) 3603–3629.
[151] L. Fan, C. Xia, F. Yang, J. Wang, H. Wang, Y. Lu, Strategies in catalysts and electrolyzer design for electrochemical CO_2 reduction toward C2+ products, Sci. Adv. 6 (2020) eaay3111.
[152] S. Liu, B. Zhang, L. Zhang, J. Sun, Rational design strategies of Cu-based electrocatalysts for CO_2 electroreduction to C2 products, J. Energy Chem. 71 (2022) 63–82.
[153] Y. Xue, Y. Guo, H. Cui, Z. Zhou, Catalyst design for electrochemical reduction of CO_2 to multicarbon products, Small Methods 5 (2021) 2100736.
[154] J. Yu, J. Wang, Y. Ma, J. Zhou, Y. Wang, P. Lu, J. Yin, R. Ye, Z. Zhu, Z. Fan, Recent progresses in electrochemical carbon dioxide reduction on copper-based catalysts toward multicarbon products, Adv. Funct. Mater. 31 (2021) 2102151.
[155] F. Hu, L. Yang, Y. Jiang, C. Duan, X. Wang, L. Zeng, X. Lv, D. Duan, Q. Liu, T. Kong, J. Jiang, R. Long, Y. Xiong, Ultrastable Cu catalyst for CO_2 electroreduction to multicarbon liquid fuels by tuning C–C coupling with CuTi subsurface, Angew. Chem. Int. Ed. 60 (2021) 26122–26127.
[156] Y. Ling, Q. Ma, Y. Yu, B. Zhang, Optimization strategies for selective CO_2 electroreduction to fuels, Trans. Tianjin Univ. 27 (2021) 180–200.
[157] G. Centi, S. Perathoner, C. Genovese, R. Arrigo, Advanced (photo)electrocatalytic approaches to substitute the use of fossil fuels in chemical production, Chem. Commun. 59 (2023) 3005–3023.
[158] C. Ampelli, D. Giusi, M. Miceli, T. Merdzhanova, V. Smirnov, U. Chime, O. Astakhov, A.J. Martín, F.L.P. Veenstra, F.A.G. Pineda, J. González-Cobos, M. García-Tecedor, S. Giménez, W. Jaegermann, G. Centi, J. Pérez-Ramírez, J. R. Galán-Mascarós, S. Perathoner, An artificial leaf device built with earth-abundant materials for combined H_2 production and storage as formate with efficiency > 10%, Energy & Environmental Science 16 (2023) 1644–1661.
[159] J. Cabana, T. Alaan, G.W. Crabtree, P.-W. Huang, A. Jain, M. Murphy, J. N'Diaye, K. Ojha, G. Agbeworvi, H. Bergstrom, S. Gersib, H. Harb, A. Stejer, G. Quiles-Galarza, O. Rodriguez, I. Caruso, J.M. Gonçalves, G.Y. Chen, C.A. Fernández, H. Pan, K. Ritter, Y. Yang, H. Zhang, A.C. García-Álvarez, S. Ilic, K. Kumar, R. Silcox, Y. Yao, H. Song, S. Stoyanov, M. Saraf, C.H. Chen, S.M.S. Subasinghe, R. Gomes, S. Lang, E. Murphy, A.S. Thind, Y. Zheng, NGenE 2022: electrochemistry for decarbonization, ACS Energy Lett. 8 (2023) 740–747.
[160] S. Zuo, Z.-P. Wu, H. Zhang, X.W. Lou, Operando monitoring and deciphering the structural evolution in oxygen evolution electrocatalysis, Adv. Energy Mater. 12 (2022) 2103383.